研究報告

高分子黏彈性的普遍性的研究(4/4)

(NSC 92-2113-M-009-027)

林銀潢教授

國立交通大學應化系

The study during the past one year has been focused on the viscoelastic behavior of polystyrene in the temperature range close to the glass-transition temperature, T_g. As schematically indicated in the Bird's-eye View of Chain Dynamics/Polymer Viscoelasticity attached in page 3, the involved dynamics and effects in this temperature range are: the motion of a single Rouse segment, the T_g-related dynamics (or the so-called α relaxation), and the loss of ergodicity. The intricacies and interplays among these physical effects as manifested by the observed thermorheological complexity are studied in detail in the two attached reports entitled (a) *Whole Range of Chain Dynamics in Entangled Polystyrene Melts from Creep Compliance*: *Themorheological Complexity between Glassy-Relaxation Region and Rubber-Fluid Region* and (b) *Motion Associated with a Single Rouse Segment versus the α Relaxation*. Some of the major accomplishments are summarized in the following:

(1) To the best of our knowledge of a dynamic system, the developed functional form enables the widest dynamic range (five decades in the magnitude of compliance or eight decades in time in one case and nine decades in another case; see Figures 1 and 2 of Report a) to be consistently quantitatively analyzed.

(2) The frictional factor K extracted from the analysis of the creep compliance $J(t)$ is in

quantitative agreement with the values obtained previously from analyzing the relaxation modulus $G(t)$ and calculated from the viscosity and diffusion data (see Table 1 of Report a)–a quantity shown independent of molecular weight as expected from the theory.

(3) Showing that the thermorheological complexity arises from the stronger temperature dependence of the energetic interactions-derived process than that of the entropy-derived ones.

(4) Revealing the physical picture at the molecular level of the effect of the loss of ergodicty on the viscoelastic behavior as the temperature is approaching the calorimetric glass-transition temperature, T_g–vitrification at the Rouse-segmental level.

(5) Showing how the length scale at T_g can be estimated by the internal yardstick provided by the Rouse-Mooney normal modes, giving 3 nm for polystyrene.

(6) The analysis of the thermorheological complexity observed in $J(t)$ of polystyrene indicates that the basic mechanism should also be responsible for the breakdown of the Stoke-Einstein relation as observed in glass-forming liquids, such as OTP and TNB, in approaching T_g from above.

(7) The study indicates that the motion associated with a single Rouse segment, as observed by depolarized photon-correlation spectroscopy, is distinctly different from the α relaxation–because of their proximity in time, the two dynamic processes could be easily confused in the past.

Dr. A. K. Das came to work in my laboratory as a post-doctor beginning in late March, 2004. He has made progresses in writing the computer programs for doing molecular-dynamics simulations. As the time period is quite short and only preliminary results have been obtained, no detailed report as to the research work being carried out by him will be made at this stage.

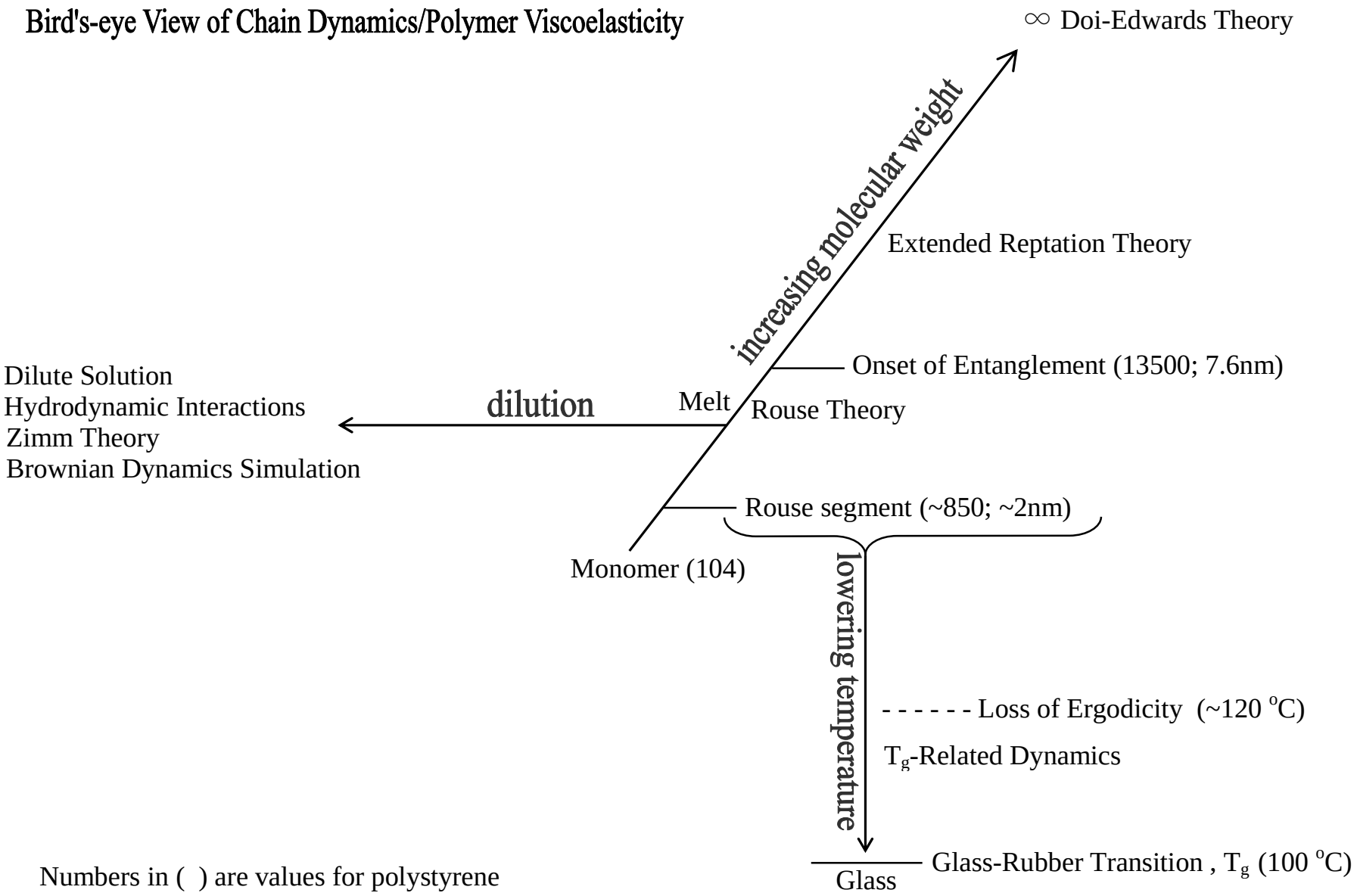
Bird's-eye View of Chain Dynamics/Polymer Viscoelasticity
∞ Doi-Edwards Theory
increasing molecular weight
Extended Reptation Theory
Onset of Entanglement (13500; 7.6nm)
Dilute Solution
Hydrodynamic Interactions
Zimm Theory
Brownian Dynamics Simulation
dilution
Melt
Rouse Theory
Rouse segment (~850; ~2nm)
Monomer (104)
lowering temperature
- - - - - - Loss of Ergodicity (~120 °C)
Tg-Related Dynamics
Glass-Rubber Transition , Tg (100 °C)
Glass
Numbers in ( ) are values for polystyrene

Whole Range of Chain Dynamics in Entangled Polystyrene Melts Revealed from Creep Compliance: Thermorheological Complexity between Glassy-Relaxation Region and Rubber-Fluid Region

Y.-H. Lin[a]
Department of Applied Chemistry
National Chiao Tung University
Hsinchu, Taiwan

Abstract

The rubber(like)-fluid region of the creep compliance $J(t)$ results reported by Plazek of two nearly monodisperse polystyrene melts in the entanglement region have been quantitatively analysed in terms of the extended reptation theory (ERT), giving the frictional factor K ($=\zeta\langle b^2\rangle/kT\pi^2m^2$) in quantitative agreement with the values obtained previously from analysing the relaxation modulus $G(t)$ line shapes as well as calculated from the viscosity and diffusion data–a quantity shown independent of molecular weight as expected from the theory. Using the successful description of $J(t)$ in terms of ERT in the rubber(like)-fluid region as the *reference frame* in time, the glassy-relaxation process $\mu_G(t)$ that occurs in the small-compliance/short-time region of $J(t)$ can be studied in perspective. As shown from the analysis in terms of a stretched exponential form for $\mu_G(t)$ incorporated into ERT, the temperature dependence of the *energetic*

interactions-derived $\mu_G(t)$ process being stronger in a simple manner than that of the *entropy-derived* ERT processes accounts fully for the uneven thermorheological complexity occurring in $J(t)$ as initially observed by Plazek. When the results of analysis being displayed in the $G(t)$ form, the relative roles of the energetic interactions-derived dynamic process and the entropy-derived ones in polystyrene are clearly revealed. It is shown that at the calorimetric glass transition temperature, T_g, the contribution from energetic interactions among segments to $G(t)$ at the time scale corresponding to the highest Rouse–Mooney normal mode greatly exceeds that derived from entropy, indicating vitrification at the Rouse-segmental level. At the same time the Rouse–Mooney normal modes provide an internal yardstick for estimating the characteristic length scale of a polymer at T_g, giving ~3 nm for polystyrene. Based on the obtained results, the basic mechanism for the thermorheological complexity occurring in polystyrene is analysed. It is shown that this basic mechanism should be also responsible for the breakdown of the Stoke -Einstein equation in relating the translational diffusion constant and viscosity as observed in glass-forming liquids, such as OTP and TNB, in approaching T_g from above.

[a] E-mail: yhlin@mail.nctu.edu.tw

Whole Range of Chain Dynamics
in Entangled Polystyrene Melts Revealed from Creep Compliance:
Thermorheological Complexity
Between Glassy-Relaxation Region and Rubber-Fluid Region

Y.-H. Lin
Department of Applied Chemistry
National Chiao Tung University
Hsinchu, Taiwan

1. Introduction

Because of the large number of atoms and degrees of freedom in a chain molecule, a polymer is rich in its dynamics, with its relaxation-time distribution easily covering many decades. For example, the time domain of the polystyrene sample with M_W=1.22x10^5 whose creep compliance $J(t)$ is analysed in this study stretches over nine decades. In general, a slow mode of dynamics corresponds to a large length scale in the chain; a fast one to a short one. It is generally understood[1] that the long-time region of the relaxation modulus $G(t)$ is sensitive to the molecular weight, coupled with entanglement; and the short-time region, with the modulus approaching that of the glass state, is sensitive to the local energetic interactions among segments. In between, there are the transition and plateau zones, which are closely related to chain entanglement (for instance, from the plateau modulus G_N one can obtain the entanglement molecular weight, $M_e=4\rho RT/5G_N$). Over the years, it has been a challenge to understand the dynamics corresponding to different length scales at a molecular level and even more so to study all of them consistently in a unified way. To analyse consistently the whole range of chain

dynamics in a unified way requires a theory that has interfaced dynamics at different length-scales seamlessly. In the past two decades, the constitutive molecular models have been developed and tested. This report represents a further progress, showing an application of what have been developed and discussing the implications of the obtained result, particularly in the understanding of the glass transition. It has been shown[2,3,4,5,6] that the Doi–Edwards theory,[7] describing the entanglement effect in terms of reptation of the primitive chain, has laid a solid foundation; and the extended reptation theory (ERT),[5,8] developed by incorporating intra-molecular Rouse-type motions into the Doi–Edwards theory, is quantitatively successful. As they have been studied in detail elsewhere, the dynamic processes in ERT will be described only briefly here. This report will first show mainly two aspects: (1) The validity of ERT is again confirmed by the analysis of the creep compliance $J(t)$ as evidenced by the obtained frictional factor K ($=\zeta\langle b^2\rangle/kT\pi^2m^2$, where ζ, b and m are the friction constant, length and mass of the Rouse segment) being in quantitative agreement with those obtained from analysing the data of relaxation modulus, viscosity and diffusion, and shown independent of the molecular weight as expected from the theory. (2) The quantitative description of the rubber(like)-fluid (or large-compliance/long-time) region of $J(t)$ in terms of ERT can be used as the *reference frame* in time, with respect to which the small-compliance/short-time region of $J(t)$ can be analysed in perspective, giving microscopic information about the dynamics closely related to the glass transition from a totally new viewpoint.

Developed on the basis of the Doi–Edwards theory, ERT gives the relaxation modulus:

$$G(t)=\frac{4\rho RT}{5M_e}F(t)\left[1+\frac{1}{4}\mu_X(t/\tau_X)\right]\left[\sqrt{M_e/M}\,\mu_B(t/\tau_B)+(1-\sqrt{M_e/M})\mu_C(t/\tau_C)\right] \quad (1)$$

with

$$F(t) = 1 + \mu_A(t/\tau_A) \qquad (2)$$

where $\mu_A(t)$ represents the Rouse–Mooney modes of motion of an entanglement strand with both ends fixed (In the short-time region, the entanglement links are regarded as fixed, cross-linked points because the chain has not had the chance to slip through the links yet. In this report, the region where the $\mu_A(t)$ process is applicable will be referred to as the Rouse–Mooney rubber region or simply as rubber region. The $\mu_A(t)$ process has often been used to represent the so-called transition zone in the literature[1]; experimentally, the transition zone should include a large portion of the glassy-relaxation process, which will be studied in this report.); $\mu_X(t)$, the chain slippage through entanglement links to equilibrate the uneven tension along the primitive chain; $\mu_B(t)$, the primitive-chain contour-length fluctuation; and $\mu_C(t)$, the reptation motion corrected for the chain length-fluctuation effect. For easy explanation as well as for referring to the research results as described in literature, the time region that covers the $\mu_X(t)$, $\mu_B(t)$ and $\mu_C(t)$ processes is grossly referred to as the rubberlike-fluid region, and that covers all the four processes $\mu_A(t)$, $\mu_X(t)$, $\mu_B(t)$, and $\mu_C(t)$ as the rubber-fluid region (see the note at ref. 9).[9] The relaxation times of these different processes are each expressed as a product of the frictional factor K and a structural factor. We refer the functional forms of the four relaxation processes and their respective characteristic (relaxation) times to the previous publications,[2-5,8] but point out that, normalizing (dividing) all the relaxation times by the relaxation time of the first mode of $\mu_A(t)$, τ_A^1, the whole $G(t)$ can be expressed as a universal function of the normalized molecular weight M/M_e.

ERT has successfully predicted the characteristics of transformation with molecular weight of the $G(t)$ line shape of the nearly monodisperse sample system; and the molecular-weight dependence of the zero-shear viscosity η and the steady-state compliance J_e^0, and their respective transition points M_c and M_c'.[2-6,8] However, the analysis of the relaxation modulus or viscoelastic spectrum in terms of ERT has been limited to the modes of motion associated with

length scales above that of a Rouse segment. The main reason is that the smallest structural unit in ERT is the Rouse segment, whose molecular weight m is estimated to be about 850 for polystyrene.[10,11,12,13,14,15,16,17,18] Experimental limitation also prevents the modes of motion faster than that of a single Rouse segment from being studied. The measurement of $G(t)$ in the high modulus region is often limited by the lack of a compliance-free transducer. Thus, in the previous studies of polystyrene,[2-5, 8] the highest modulus that could be studied was about 10^7 dynes/cm^2, which is of the magnitude a little smaller than that corresponding to m=850.[12-14] On the other hand, the creep experiment based on the use of the frictionless magnetic bearing by Plazek allowed the creep compliance $J(t)$ as small as ~10^{-10} cm^2/dyne to be measured accurately.[19,20] These small measurable compliance values correspond to the large modulus values of reciprocal magnitude. As ERT can be used to analyse quantitatively the relaxation modulus $G(t)$ of magnitude smaller than ~10^7 dynes/cm^2, it is expected to describe well the creep compliance $J(t)$ in the large-compliance/long-time region. From the analyses of the relaxation-modulus curves of a series of nearly monodisperse polystyrene samples of different molecular weights in terms of ERT, the obtained frictional factor K is shown to be independent of molecular weight. This result is critically important to ERT, indicating that the functional forms of the dynamic processes as arranged in eqs.1 and 2 as well as the structural factors of their respective relaxation times are accurately given. Thus, with both the molecular weight and entanglement molecular weight M_e known (M_e determined independently from the plateau modulus $G_N=4\rho RT/5M_e$), the analysis of the large-compliance/long-time (rubber(like)-fluid) region of $J(t)$ in terms of ERT is boiled down to the determination of the single parameter K.[21]

The small-compliance/short-time region of $J(t)$ reflects the fast local segmental motions, which are much affected by the strong energetic interactions among segments. In this region of $J(t)$ with compliance comparable to that of the glass state, the dynamic process is much related to the glass transition of the polymer. It is often referred to as the glassy relaxation. In the case of polystyrene, it has been shown by Plazek[19,20] that as the temperature is close to the glass

transition temperature–below ~ 120^{o} C–the time-scale shift factors of the $J(t)$ curves with temperature in the softening (glass-rubber) region become greater than in the rubberlike-fluid region. As the viscosity is dominated by the terminal relaxation process, such an effect was also demonstrated by the divergence of the temperature dependences of the viscosity and recoverable compliance $J_r(t)$ as the temperature decreases below 120^{o}C. This difference in temperature dependence means that the principle of thermorheological simplicity breaks down between the rubberlike-fluid region and the glass-rubber region in this low-temperature range. As will be shown in this report (see Figure 4), the rubber region in $J(t)$ is under the influence of the glassy relaxation; the thermorheological complexity actually occurs between the glassy-relaxation process and the processes in the rubber-fluid region, instead of between glass-rubber region and the rubberlike-fluid region (see the note at Ref. 9 for explanations for the term "rubber(like)" used in this report, which is related to this effect). The thermorheological-complexity phenomenon not only is interesting but also should be important for our understanding of the glass transition. Using the quantitative description of the rubber(like)-fluid region of $J(t)$ in terms of ERT as the reference, the glassy-relaxation process at different temperatures are characterized quantitatively and consistently in this study. In this way, the whole range of chain dynamics–covering motions corresponding to sub-nano-scales, the Rouse-segmental length (~2nm), the entanglement distance (7.6 nm) and the length scale of the whole molecule ($\gtrsim$14 nm for sample A; $\gtrsim$23 nm for sample B)–is revealed. The results of analysis at different temperatures are displayed in the $G(t)$ form. Through the molecular picture as contained in ERT, the basic mechanism for the thermorheological complexity is analysed, and the relation between the thermorheological complexity and the glass transition is studied.

2. Calculation of Creep Compliance

The creep compliance is related to the relaxation modulus by the convolution integral:

$$t = \int_0^t J(t')G(t-t')dt \qquad (3)$$

With $G(t)$ known, $J(t)$–the target function–can be calculated from Eq. (3). The convolution integral may be solved numerically by the method of Hopkins and Hamming.[22,23] In this method, the interval of integration is divided into subintervals which are small enough so that a mean value of the target function over the subinterval can be taken outside of the integral. In this way, a recursion relation can be set up, from which the target function eventually emerges as a discrete set of values. In the case, as done in the present report, where equal spacing in log t is used for choosing the subintervals, transient-viscosity quantities used in the recursion equation need to be evaluated first by the interpolation procedures as detailed in ref. 23. In calculating the $J(t)$ curves shown in this report, using ten points per decade in time is sufficient, as no difference can be discerned in the comparisons with curves calculated with a much higher resolution.

To incorporate the glassy-relaxation process into ERT, eq 2 is replaced by the following equation

$$F(t) = 1 + \mu_A(t/\tau_A) + A_G\mu_G(t/\tau_G) \qquad (4)$$

where $\mu_G(t)$ represents the glassy-relaxation process and A_G is its relaxation strength. In using eq 4, it is expected that $\mu_G(t)$ is a much faster process than the normal-mode processes in $\mu_A(t)$; the fast local segmental motions in $\mu_G(t)$ can be regarded as the sources of the random fluctuation forces in the Langevin equation from which $\mu_A(t)$ is derived.[5,8, 24,25] As shown below, this is true except when the temperature is basically at the glass transition temperature, where the loss of effective ergodicity is expected to occur; therefore, the applicability of the Langevin equation should be questioned. The number of normal modes N_e in the $\mu_A(t)$ process is set to be 16 corresponding to the mass of a Rouse segment, m, being about 850[10-18] and the entanglement

molecular weight M_e=13500.[2,4,5]

In this study, it has been found that the glassy-relaxation process can be well described by the stretched exponential form

$$\mu_G(t/\tau_G) = \exp\left[-(t/\tau_G)^{\beta}\right]; \quad 0 < \beta \le 1 \qquad (5)$$

For a relaxation process as given by eq 5, the average relaxation time is defined by

$$\langle\tau\rangle_G = \int_0^{\infty} \mu_G(t/\tau_G)dt = \frac{\tau_G}{\beta}\Gamma(1/\beta) \qquad (6)$$

where Γ is the gamma function. In the whole relaxation-time distribution, the glassy-relaxation region is situated in a certain position relative to the rubber(like)-fluid region, where all the relaxation times are proportional to the frictional factor K.[26] We may express the relative position by

$$\langle\tau\rangle_G = s\,K \qquad (7)$$

where s is a proportional constant and has the unit of Dalton square. Although s is not unit-less, it can be regarded as a "normalized" glassy-relaxation time, as it represents the glassy-relaxation time with K fixed at 1 or any constant. In the neighbourhood of T_g, the parameter s increases with decreasing temperature, reflecting the thermorheological complexity between the glassy-relaxation region and the rubber-fluid region.

As shown below (Section 3.1), the line shape of $J(t)$ in the rubber(like)-fluid region is well described by ERT as expected, allowing the K value to be determined. The whole $J(t)$ curve can be calculated with A_g, β, and s as contained in eqs 4, 5, 6 and 7 as the adjustable parameters

for fitting to the line shape in the short-time/small-compliance region (<~ 5×10^{-7} cm^2/dyne) of the measured $J(t)$. In the initial stage, we are mainly concerned with the line shape of $J(t)$; in the fitting process, we calculate the whole $J(t)$ curve at some fixed K value and allow it to shift along the time coordinate to fit to the $J(t)$ result measured at a certain temperature. After good fitting over the whole time range of the $J(t)$ result has been obtained, the absolute value of K for the temperature can be calculated from the shift factor. Different parts of $J(t)$ in the small-compliance region are sensitive to these individual parameters in greatly different degrees. Specifically, with a properly chosen A_G value which will give the observed glassy compliance, $J_g=\lim_{t\to 0} J(t)\sim 10^{-10}$ cm^2/dyne, β affects the $J(t)$ line shape virtually only in the small-compliance region, < 10^{-8} cm^2/dyne. The region, $10^{-8}\sim5\times10^{-7}$ cm^2/dyne, while being insensitive to a change in β, is determined by the product of A_G and $\langle\tau\rangle_G$ or A_G and s with K being fixed; in other words, it is directly related to the integration area of $A_G\,\mu_G(t)$. Since A_G is very much dictated by the J_g value of the studied sample and can be easily quantified, the position in time of the glassy-relaxation region relative to the rubber(like)-fluid region can be used to determine the s value. Under the condition that a particular measured curve (at a certain temperature of measurement) and the calculated curve are matched, while the shifting factor along the time coordinate obtained from the matching allows the K value to be calculated, the s value can be determined uniquely by monitoring the agreement between the calculated and measured curves in the β-insensitive region, 10^{-8} ~ 5×10^{-7} cm^2/dyne. With the s value determined this way, the β value can then be determined by comparing the calculated curve with the measured in the small-compliance region, < 10^{-8} cm^2/dyne. Following the above described procedure, a set of the parameters: A_G, β and s can be uniquely determined for the system at a certain temperature. While A_G and β are very much independent of temperature, s increases significantly with decreasing temperature.

3. Comparison with Experimental Results

3.1. Creep Compliance Curves. Plazek has reported the creep-compliance results of two nearly monodisperse polystyrene samples in the entanglement region,[19,20] denoted by A and B here: A with $M_w = 4.69\text{x}10^4$ and B with $M_w = 1.22\text{x}10^5$. Even though the samples are nearly monodisperse, eq 1 need be convoluted with their molecular weight distributions to calculate $G(t)$ and then $J(t)$ for comparison with experimental results. The convolution only affects the rubberlike-fluid region. As shown previously,[2-5] the Schulz distribution[27] should be a good representation of molecular-weight distribution for samples like A and B. The polydispersity of the Schulz distribution is characterized by the single parameter Z ($M_w/M_n=(Z+1)/Z$). In the present analysis of $J(t)$, Z is used as an adjustable parameter. Close agreements between the calculated and measured $J(t)$ curves have been obtained with Z=20 for both samples, corresponding to M_w/M_n=1.05.

From the analyses of the $G(t)$ curves of a series of polystyrene samples of different molecular weights, with M_e=13500 calculated from the plateau modulus $G_N=2\text{x}10^6$ dyne/cm^2, the frictional factor K is found to be independent of molecular weight to as low as just above M_e and is determined to be $4.7\text{x}10^{-9}$ within a small experimental error at 127.5^{o}C (see Table 1).[2,5] As shown in Figures 1 and 2, the $J(t)$ curves of samples A and B measured at different temperatures are compared with the curves calculated, through eq 3, from the $G(t)$ calculated on the basis of the combination of eqs 1, 4, 5, 6, and 7 with $K=5\text{x}10^{-9}$ and $G_N=2\text{x}10^6$ /1.057. The factor 1.057 in the G_N value used is the ratio of the product of density ρ and absolute temperature T between 127.5^{o}C and 100^{o}C; it is used here for convenient comparison of the calculated $J(t)$ curves with Plazek's results which have all been reduced along the compliance axis by the factor $\rho T/\rho_o T_o$ using 100^{o}C as the reference point (see Figure 1 of ref. 19 and Figure 7 of ref. 20). Thus, Figures 1 and 2 use a mixed reference system: 100^{o}C as the reference temperature for the compliance coordinate and 127.5$\pm$0.4^{o}C for the time coordinate.[28,29] The shown fittings between the calculated and measured $J(t)$ curves are done by visual superposition with the aid of a graphical software.[30] Being wavy, each $J(t)$ curve has three bending points: two concaves and

one convex as shown in the figures. Because each bending point basically denotes a position in the two-dimensional plot of log $J(t)$ vs. log t, the matching between the calculated and measured curves around each bending point allows one to determine the absolute value of compliance (reduced to 100^{o}C and thus is independent of temperature) and the relative value of time (dependent on temperature). And the simultaneous matching over two bending points is a key criterion for determining the line shape of $J(t)$. In the shown close agreements between the calculated and measured $J(t)$ curves, for sample A no shift along the J axis is required for all the curves; for sample B no shift along the J axis is required at 105.5, 101.0 and 98.3^{o}C, while a shift of the experimental data upwards by ~5% is made (for a slightly better agreement than can be achieved without making such a shift) at 119.8 and 113.8^{o}C. All the agreements in line shapes as shown in Figures 1 and 2 involve two bending points except at the lowest temperatures, 97 and 98.3^{o}C for samples A and B, respectively. At these two lowest temperatures, since the parameters A_G and β are well determined by the good fittings at other temperatures, the s values determined from the close agreements between the calculated and measured in the very low-compliance region, even though around only a single bending point, should be dependable as well. This is confirmed in the accompanying paper [31] and by the consistency between the composition of the $J(t)$ curves measured at different temperatures as shown in Figure 1 and that shown in Figure 2 of ref. 19.[32] (see the note at ref. 32)

For all the calculated curves in close agreements with the measured results as shown in Figures 1 and 2, the A_G values are 5482 and 4119 giving J_g= 7.69x10^{-11} and 1.02x10^{-10} cm^2/dyne for sample A and sample B, respectively, while β=0.41 for both samples. The difference in A_G between samples A and B is directly related to their difference in J_g, which is quite apparent by a visual examination of the experimental results. The larger J_g of sample B should be due to the presence of residual plasticizers which was regarded by Plazek[20] as the cause for its smaller values and weaker temperature dependence of viscosity at temperatures close to T_g in comparison with a normal polystyrene sample of comparable molecular weight (see Figure 11 of

ref. 20). This association is further confirmed by the smaller frictional factors extracted from the $J(t)$ line-shape analysis for sample B as shown in the next section. Because the plasticizer molecules are very mobile, their presence in sample B will cause a fast relaxation process of very small relaxation strength to occur in $G(t)$, and in effect gives rise to some additional free volume Thus, the residual plasticizers in sample B have the effect of reducing somewhat the glassy compliance–as clearly visible in the $J(t)$ results of Plazek– as well as the value of the frictional factor K. However, the entanglement molecular weight is virtually not affected at all because there is only a residual amount of the plasticizer. As a result, the interrelations (ratios) among the relaxation times τ_A, τ_X, τ_B, and τ_C which are determined only by the structural factors–functions of the normalized molecular weight M/M_e–are not affected;[2-5,8] in other words, the line shape of the viscoelastic spectrum over the rubber-fluid region will not be affected. As A_G is reduced by about 25% by the residual mobile plasticizer molecules, the glassy-relaxation region in sample B will be directly affected. However, as the discrepancy is only 25%, some of the information obtained from the $J(t)$ line-shape analysis of sample B can still be used; clearly the K value obtained from sample B cannot be used. This will be further discussed below over the results obtained from analysing the $J(t)$ data.

3.2. Frictional Factor, *K*. For sample A, the frictional factor K at 127.5^{o}C can be first calculated from the time-scale shift factor obtained from superposing the calculated $J(t)$ curve on that measured at 125^{o}C as described in Section 2 and then corrected for the temperature difference between 127.5 and 125^{o}C using the temperature dependence of its viscosity.[19,29] In this way, K=4.8x10^{-9} is obtained in quantitative agreement with those determined from the analyses of the $G(t)$ results as reported before and mentioned above as well as those calculated from the viscosity[29] and diffusion[33,34,35] data. The agreement of the K values as shown in Table 1 (see the Appendix as well) is significantly rigorous, considering the constancy of K over a wide range of molecular weight and that these K values are obtained from analysing experimental results measured independently by totally different kinds of instruments–strain-controlled vs.

stress-controlled rheometer–and of quantities of different nature–viscoelasticity vs. diffusion.

For sample B, the frictional factor at 127.5^{o}C can be calculated first from the time-scale shift factor obtained from the superposition of the calculated with the $J(t)$ curve measured at 134.5^{o}C or at 119.8^{o}C and then corrected for the temperature difference using the temperature dependence of the viscosity of a normal (uncontaminated) polystyrene sample with a comparable molecular weight.[29] We obtain K=3.7 x10^{-9} if through 134.5^{o}C and K= 3.0x10^{-9} if through 119.8^{o}C. Both these two values are somewhat smaller than that for a normal sample, particularly the latter, supporting the presence of residual plasticizers in sample B. Furthermore, the presence of residual plasticizers in sample B has a larger effect, as in comparison with a normal sample, on its viscosity or frictional factor at a temperature close to T_g than at a higher temperature. This is the reason, to which Plazek attributed the smaller values and weaker temperature dependence of the viscosity of sample B in the temperature region close to T_g.[20] This is clearly also reflected by the smaller K value of sample B obtained through 119.8^{o}C than through 134.5^{o}C.

Due to the presence of residual plasticizers in sample B, as pointed out above, the K values obtained from sample B cannot be included in Table 1, which shows the molecular weight independence of K . In the accompanying paper,[31] the obtained K values for sample A from 127.5 to 97^{o}C are listed in Table 1; the consistency between the temperature dependence of K and that of viscosity (as $\eta/\rho T$) is shown in Figure 5.

3.3. Thermorheological Complexity. The thermorheological complexity as first pointed out by Plazek [19,20,36] in reporting his $J(t)$ results is shown caused by the increase of the normalized glassy-relaxation time s with decreasing temperature. The s values that give the close fittings between the theory and experiments as shown in Figures1 and 2 are shown as a function of temperature for both samples together in Figure 3. These two molecular-weight dependence curves of s are parallel with each other indicating a similar effect taking place in both the systems. Over the shown temperature range, s increases by about an order of magnitude with

decreasing temperature. One can basically superpose the curve of sample A onto that of sample B by multiplying the *s* values of sample A by a factor of 2.6.

While the frictional factor *K* in the $\mu_X(t)$, $\mu_B(t)$ and $\mu_C(t)$ processes is independent of molecular weight to as low as just above M_e (see the Appendix), the frictional factor in the $\mu_A(t)$ process denoted by K' has been found to have a plateau value ~3.3*K* in the high molecular-weight region, start to decline at $M/M_e \sim 10$ with decreasing molecular weight, and become identical to *K* as $M/M_e \to 1$.[2,5] The same molecular-weight dependence of K/K' is also observed for the blend-solution system [4,5] when it is expressed in terms of the normalized molecular weight: M/M_e for the pure melt and M/M_e' for the blend solution ($M_e' = M_e W^{-1}$ where *W* is the weight fraction of the entangled component; see the note at ref. 37).[37] The dependence of K'/K on M/M_e (or M/M_e') can be described by the empirical equation.[4,5]

$$\frac{K'}{K} = \frac{2.525}{\exp\left[-0.643\left(\frac{M}{M_e} - 4.567\right)\right] + 1} + 0.769 \qquad (8)$$

The dependence of K'/K on M/M_e has been explained before and will be further discussed below with respect to the results obtained in this study. As calculated from eq 8, $K' = 1.61K$ for sample A; $K' = 3.16K$ for sample B. These two K' values differ by a factor of 1.96. This ratio is close to that between the *s* values obtained for samples A and B at the same temperature. Since the product of A_G and *s* is what matters in determining the *s* value as explained in Section 2, the difference between 2.6 and 1.96 is most likely related to the A_G value for B being somewhat smaller that that for A; indeed, the product of 5482 (A_G of sample A) and 1.96–the expected normal situation–is very close to that of 4119(A_G of sample B) and 2.6–the situation disturbed by the presence of residual plasticizers. The presence of residual plasticizers affects the line

shape in the glassy-relaxation process region of sample B somewhat. As the distortion of the A_G $\mu_G(t)$ line shape is not large, the comparison of the two sets of results can still reveal that the dynamics of the whole $\mu_G(t)$-$\mu_A(t)$ region, not limited to the $\mu_A(t)$ process, are characterized by relaxation times depending on molecular weight in the same way as K'(or K'/K as given by eq 8). This will be more clearly illustrated below (Section 4.2) in the comparison the $G(t)$ line shapes in the glassy-relaxation region between samples A and B.

3.4. Fitting Parameters. It is advisable at this point to summarize the parameters involved in the theoretical fitting to the $J(t)$ line shapes of samples A and B as described above and discuss their uniqueness and significance. The relevant parameters involved in describing the $J(t)$ line shapes over eight decades in time in one case and over nine decades in the other case are A_G, β, s (or either τ_G or $\langle\tau\rangle_G$), M_e, K, K'(or K'/K), Z and m. Among these parameters, most have been predetermined:

The entanglement molecular weight M_e has been determined independently from the plateau modulus–a static property. An error in the M_e value will lead to an error in the obtained K value because both M_e and K appear in the equations for the relaxation times τ_A, τ_X, τ_B, and τ_C; thus, an accurate determination of M_e is essential. M_e=13500 has been obtained from the convergence in consistence of the assumed M_e value with the plateau modulus value obtained in the least-square fitting process of the quantitative $G(t)$ line-shape analysis.[2,4,5] This M_e value is also confirmed by the close agreement with the value 13300 determined by the integration method.[38]

With the accurately determined M_e, the frictional factor K was found independent of molecular weight from an extensive $G(t)$ line-shape analysis. In the $G(t)$ line-shape analysis, the polydispersity of the studied nearly monodisperse samples need be considered. The polydispersity parameter Z values obtained from the $G(t)$ line-shape analyses are extremely well-behaved; they fall between Z=30 and 120 corresponding to M_w/M_n=1.03 ~ 1.01, well within the range expected for a nearly monodisperse sample. The Z parameter affects mainly only the

shape of the $G(t)$ curve in the terminal region; any possible small uncertainty in Z virtually has no effect on the obtained K value. Thus, the obtained molecular-weight independence of K is virtually not affected by the polydispersity variation among the studied nearly monodisperse samples.

The dependence of the K'/K ratio on molecular weight as phenomenologically described by eq 8 was determined from the relative position of the $\mu_A(t)$ process region to the plateau-terminal region by the $G(t)$ line-shape analyses.[2,4,5]

The molecular weight m of a Rouse segment, which determines the number of normal modes in $\mu_A(t)$, mainly affects the interface region between the energetic interactions-derived dynamic process ($A_G\mu_G(t)$) and the entropy-derived dynamic processes (the ERT processes: $\mu_A(t)$, $\mu_X(t)$, $\mu_B(t)$ and $\mu_C(t)$). The $A_G\mu_G(t)$ process and the ERT processes are of different nature; thus, a discontinuity occurring at the interface between the two intrinsically different kinds of dynamic processes is not surprising. Using eqs 1, 4 and 5 for the line-shape analysis, we have substituted a discontinuity for a somewhat smoother transition as should most likely occur in reality. The discontinuity picture can be considered as a first-order approximation and should work well if the location of discontinuity as represented by the m value is properly chosen. m=850 falls within the range of the values determined by various techniques[10-18] with small variations. The discontinuity approximation and the proper choice of m are supported by the extensive close agreements between the calculated and measured $J(t)$ curves as shown in Figures 1 and 2.

The facts that the K value obtained for sample A at 127.5°C agrees closely with the values obtained previously (see Table 1) and that the obtained Z value (=20; corresponding to M_w/M_n=1.05) is well within the expected range allow us, to the same effect, to regard K and Z along with M_e, K' (or K'/K as given by eq 8) and m as predetermined parameters. In other words, A_G, β and s are the main fitting variables in this study, affecting the small-time/small-compliance region of $J(t)$. The end result is the seamless quantitative description of $J(t)$ over the whole time

range. Here, it should be stressed that the foundation for the quantitative description of $J(t)$ is ultimately K being independent of molecular weight. Because of the success of ERT as represented by the molecular-weight independence of K, theoretically, there is no limit to the time range of $J(t)$ that can be analysed, depending on the molecular weight of the sample under study.

Among the three variables A_G, β and s, as indicated above, A_G is basically dictated by the glassy modulus–the reciprocal of the glassy compliance J_G–and β is only sensitive to the $J(t)$ line shape in the small-compliance region, $<10^{-8}$cm^2/dyne. Thus, the determination of the best values for A_G and β is effectively decoupled from that of s, which reflects the shift with temperature of the $J(t)$ curve in the 10^{-8}~$5\text{x}10^{-7}$ cm^2/dyne region along the normalized time coordinate (In this study, the time coordinate under a fixed K value, as chosen to be $5\text{x}10^{-9}$ in Figures 1 and 2, is regarded as a normalized time coordinate). The whole thermorheological complexity in $J(t)$ is reduced to the simple change in s with temperature shown in Figure 3. This reduction is of particular significance as we can notice in Figures 1 and 2 that the shift with temperature in the ~$5\text{x}10^{-7}$ cm^2/dyne region is not as large as that in the ~10^{-8} cm^2/dyne region. The thermorheological complexity in $J(t)$, even though being temporally uneven, is fully explained by the simple change in s, which, very importantly, has a clear physical meaning, namely representing the stronger temperature dependence of the energetic interactions-derived dynamic process than that of the entropy-derived ones. The mechanism how the temporal unevenness of the thermorheological complexity is related to the simple change in s will be shown in Section 4.1.

Thus, although in the appearance there are 8 parameters involved in calculating the $J(t)$ curves in quantitative agreement with the measured ones over the whole time range, the whole thermorheological complexity in $J(t)$ is uniquely represented by the simple change in s with temperature as all the other parameters can be determined independently beforehand or from the $J(t)$ line-shape analysis in a specific region.

It is advisable here to comment on the large dynamic range revealed by the $J(t)$ line-shape analysis–6 decades–as shown in Figures 1 and 2, which should be rare, if even been done. Two main reasons make this wide range of analysis possible: The first is the consistently accurate $J(t)$ data of Plazek over a wide dynamic range, covering four decades in a single creep run in the best cases. The second is the correctness of the ERT-based functional form used to analyse the $J(t)$ data; the close agreement between the calculated and measured guides the overlapping and correlation of the $J(t)$ data measured at different temperatures, which extends one decade of dynamic range (see the note at ref. 32). Then, the theoretical equation allows the results of analysis to be extended for another decade in the flow region.

To put the combination of eqs 1, 4 and 5 in a proper perspective, it may be pointed out that while ERT is a molecular theory, the inclusion of $A_G\mu_G(t/\tau_G)$ as defined by eqs 4 and 5 is a phenomenological description. Using the stretched exponential form characterized by the three parameters A_G, β and τ_G is a common practice in describing a observed dynamic process closely or directly related to the glassy-relaxation process of a glass-forming polymer or liquid[39,40] In fact, being described by a stretched-exponential form is considered as one of the canonical features of the T_g-related dynamic process. Even though it is generally understood that the three parameters: A_G, β and τ_G, are closely related to the energetic interactions among the molecules or polymer segments, there is currently no molecular theory for relating them. Although we don't have the microscopic knowledge of the three parameters, from the results obtained from the $J(t)$ line-shape analysis, particularly the change in s with temperature, an informing *large picture* of the polymer dynamics can be revealed as discussed below.

4. Discussion

4.1. Comparison of $J(t)$ and $G(t)$. Shown in Figure 4 is the comparison of the curves of log $G(t)$ and log $J(t)^{-1}$ vs. log t calculated with K=5x10^{-9} at the s value corresponding to 113.8^{o}C for sample B. One can see that the $G(t)$ curve has clear line-shape features showing the separate

processes as given in eqs 1 and 4, while the solution of the convolution integral (eq 3) for calculating $J(t)$ "smears" the separate features greatly. To illustrate this, both the $G(t)$ and $J(t)$ curves calculated without the contribution of the $A_G\mu_G(t)$ process are shown for comparison with the full curves. One can see that the influence of the $A_G\mu_G(t)$ contribution in $J(t)$ extends to the time region corresponding to the $\mu_A(t)$ process; in contrast, the $A_G\mu_G(t)$ and $\mu_A(t)$ processes in $G(t)$ are localized in the individual time regions where they occur and are well separated. Thus, the stronger temperature dependence of the $\mu_G(t)$ process can much affect $J(t)$ in the time region corresponding to the $\mu_A(t)$ process. In other words, in $J(t)$ the effect of the increase in s with decreasing temperature extends to the region around ~$5\text{x}10^{-7}$ cm^2/dyne instead of being only localized in the time region of the glassy relaxation $\mu_G(t)$. As the effect diminishes gradually with time scale, the temperature dependence in the region around ~$5\text{x}10^{-7}$ cm^2/dyne is not as strong as that in the glassy-relaxation region–this is the temporal unevenness of the thermorheological complexity in $J(t)$ as pointed out above. The unevenness has been first observed by Plazek[20] (see Figure 9 of ref. 20) in saying "The divergence seen in the region of the 'knee' of the reduced (recoverable compliance) curve indicates that all of the retardation mechanisms do not have the same temperature dependence." Indeed, this observation is an unusual discovery as Plazek stated "This discrepancy would not have been detected without a large range of time scale." However, without the help of a valid molecular theory as the base, this observed phenomenon has not been given a full explanation for more than thirty years. Here, we show that the intricacy arises mainly from the smearing effect of going through the convolution integral in eq 3 and that the source of the whole phenomenon is traced back to a rather simple physical effect.

In the case of sample A the glassy-relaxation process has a small yet basically negligible effect on the flow region of $J(t)$ as well, because its terminal region is relatively not that far away due to its smaller molecular weight. The effect becomes more obvious as s becomes larger with decreasing temperature. (see Figure 1)

4.2. Thermorheological Complexity as Displayed in $G(t)$. As shown in this study, in spite of the smearing effect in $J(t)$, the whole range of the $J(t)$ curves can be analysed in the framework of ERT into which $A_G\mu_G(t/\tau_G)$ is incorporated, revealing the dynamics in different time regions. Using the results obtained from the analysis of $J(t)$, the hierarchy of the dynamic processes can be displayed in the $G(t)$ form for a clearer discussion. In Figures 5 and 6, we show the $G(t)$ curves calculated with $K = 5\text{x}10^{-9}$ for samples A and B, respectively, at the s values corresponding to 114.5, 104.5 and 97°C for A and 113.8, 105.5 and 98.3°C for B. In these figures, the curves calculated without the contributions of $A_G\mu_G(t)$ and without both of $A_G\mu_G(t)$ and $\mu_A(t)$ are also shown. The differences between these curves correspond to the separate contributions of the $A_G\mu_G(t)$ and $\mu_A(t)$ processes. In these figures, the locations of the relaxation times, $\langle\tau\rangle_G$, τ_A^p (for the normal modes of $\mu_A(t)$; p=1,2...15), τ_X, τ_B, and τ_C are also indicated. The number of normal modes used for $\mu_A(t)$, i.e. $N_e-1=15$, is a very reasonable choice as it corresponds to the mass for a Rouse segment, m, to be about 850, which falls within the range of the values determined by various techniques with small variations.[10-18] Segmental motions within a chain section shorter than 850 is regarded as belonging to the glassy relaxation. From the $\{\tau_A^p\}$ points shown in Figures 5 and 6, one sees that the relaxation times of the high Rouse–Mooney modes are closely packed; in choosing the number of modes, to differ by one or two basically does not affect the main point that we shall make and discuss below.

τ_A^{15} is the relaxation time of the fastest among the modes that contribute to the modulus of entropy origin; it can be regarded basically as the motional time constant associated with a single Rouse segment τ_v. Thus, it is a key time constant for comparison with $\langle\tau\rangle_G$. As shown in Figures 5 and 6, the $\langle\tau\rangle_G$ values at the shown temperatures are all much shorter than τ_A^{15} for both samples A and B. The great disparity between $\langle\tau\rangle_G$ and τ_A^{15} appears basically consistent with the stochastic assumption in the Langevin equations, from which the theoretical expression of $\mu_A(t)$ is derived. At the highest shown temperatures (114.5°C for A and 113.8°C for B), the modulus due to $A_G\mu_G(t)$ has basically relaxed to a negligible level at $t=\tau_A^{15}$ (G/R=0.05 and 0.12,

respectively, where G is the glassy contribution, calculated from the $A_G\mu_G(t)$ term; and R is the rubbery contribution, the sum of the remaining terms). The validity of the Langevin equations should hold well here. At the intermediate temperatures (104.5°C for A and 105.5°C for B), the contributions arising from energetic interactions among segments and derived from entropy are of the same order of magnitude at $t=\tau_A^{15}$ (G/R=0.96 and 1.3, respectively), indicating that the ergodic assumption behind the Langevin equations may become not totally valid. As the temperature decreases basically to the calorimetric T_g (at 97°C for A and 98.3°C for B), the contribution to the total modulus from the energetic interactions greatly exceeds the entropy-derived contribution at $t=\tau_A^{15}$ (G/R=11.7 and 9.8, respectively), indicating vitrification at the Rouse-segmental level. At these low temperatures, the full validity of the Langevin equations should be questioned, even though $\langle\tau\rangle_G<\tau_A^{15}$. In this situation, the combination of the functional forms given for $A_G\mu_G(t)$ and $\mu_A(t)$ can be considered as a good phenomenological representation for the processes in the short-to-intermediate time region of $J(t)$ However, $\mu_A(t)$ can be regarded as what the Rouse–Mooney modes of motion would be if the glassy-relaxation process had not moved to longer times in the normalized scale. Thus, what is shown at $\sim T_g$ in Figures 5 and 6 does not only tell us that at $t\sim\tau_A^{15}$ the rubbery elasticity has been overshadowed or basically replaced by the energetic interactions-based elasticity but also allows us to use the relaxation times of the various Rouse–Mooney modes as "graduations" of a yardstick for estimating the extent of the influence of the glassy-relaxation process.

In terms of $G(t)$, we can more directly illustrate the small distortion of the $A_G\mu_G(t/\tau_G)$ line shape by the residual plasticizers in sample B and further make it clear that the distortion does not really affect what can be revealed–namely, the ratio between samples A and B of the relaxation times in the whole $\mu_G(t)$-$\mu_A(t)$ region, not limited to the $\mu_A(t)$ process, follows that of K' (or K'/K as given by eq 8). The two sets of $G(t)$ curves as shown in Figures 5 and 6 have approximately the same one-to-one corresponding temperatures: 114.5 vs. 113.8; 104.5 vs. 105.5; and 97 vs. 98.3. Both 97 and 98.3 are each close to the T_g of samples A and B,

respectively.[41,42,43] The *G/R* ratios at the three corresponding temperatures being basically of the same magnitude: 0.05 vs. 0.12; 0.96 vs. 1.3 and 11.7 vs. 9.88, clearly indicate that the dynamics of the whole $\mu_G(t)$-$\mu_A(t)$ region, not limited to the $\mu_A(t)$ process, are characterized by relaxation times depending on molecular weight in the same way as *K'*. In fact, allowing for ~±25% deviations between two corresponding curves, which can account for the difference in A_G between samples A and B as well as the small differences in temperatures, the two sets of $G(t)$ curves as shown in Figures 5 and 6 can basically superpose on each other in the whole $\mu_G(t)$-$\mu_A(t)$ region rather well with a shift factor of ~2 along the normalized time coordinate, expected from the ratio of *K'/K* between the two samples. In comparison with this factor, a 25% deviation is rather small; in other words, the above drawn conclusion is sound.

The separation of the energetic interactions-derived dynamic process $A_G\mu_G(t/\tau_G)$ and the entropy-derived ones with the former having a stronger temperature dependence as shown in Figures 5 and 6 is consistent with the separation of the glassy and rubbery components of the dynamic Young's modulus spectra by Inoue *et al*.[12,13] analyzing dynamic mechanical and birefringence results (see Figure 7 of ref. 12). However, the spectra of the rubbery component of Inoue are limited to the $\mu_A(t)$-process region and the early part of the plateau region by the nature of their experiment. As shown in the accompanying paper,[31] the obtained temperature dependences of τ_A[15] (equivalent to that of *K*) and $\langle\tau\rangle_G$ are, respectively, in close agreement with those of the viscosity and recoverable compliance obtained by Plazek.[19,29] At the same time, the temperature dependence of the rubbery component and that of the glassy component separated by Inoue *et al*. are shown to be in agreement, respectively, with those of the viscosity and recoverable compliance of Plazek in ref. 13. Thus, the present study shows the consistency between the results of Plazek and Inoue *et al*. in both the forms and temperature dependence. Such a link can be made, because, as opposed to the usual data reduction as used by Plazek and Inoue *et al*., key parameters are obtained from the analysis of the $J(t)$ data in terms of eqs.1, 4 and 5, which allow the results to be recast in any viscoealstic form (see the Appendix of ref. 31).

4.3. Comments based on Literature Results of the Transition Zone. In general, it has often been indicated that the relaxation in the transition zone is independent of molecular weight[1]. However, this is based on the results obtained in the high-molecular-weight region where, as indicated by eq 8 for polystyrene, K'/K is independent of molecular weight (above ~ $10M_e$). In fact, the raw $J(t)$ data of Plazek show that at the same temperature sample B reaches the same compliance level in the small compliance region, say at 10^{-9}cm^2/dyne, significantly later than sample A even though sample B is contaminated by residual plasticizers. The ratio between the two time values is estimated to be roughly that obtained above, ~2, after their difference in K is taken into account–note: both Figures 5 and 6 are displayed under the same K=5x10^{-9}. The similar molecular-weight dependence of the transition zone (the $\mu_G(t)$-$\mu_A(t)$ region) is also observed in other polymers. For instance, in the $J(t)$ results of poly(cis-isoprene) obtained by Nemoto et al[44]: the transition region ($J(t)$ curve from $\lesssim 10^{-9}$ to $\gtrsim 10^{-8}$ cm^2/dyne; see Figure 1 of ref. 44) of a sample with molecular weight at ~ $1.4M_e$ occurs earlier by a factor of ~4.5 than those at higher molecular weights (>$4M_e$),[45] which show very weak molecular-weight dependence. The similar effect also occurs in the $J(t)$ results of poly(vinyl acetate) obtained by Ninomiya and Ferry[46]: the transition region ($J(t)$ curve from $\gtrsim 10^{-9}$ to $\lesssim 10^{-7}$ cm^2/dyne) of a sample at ~ $1.5M_e$ occurs earlier by a factor of ~2.5 than that in the high molecular-weight limit. All these results indicate that all the relaxation processes in the transition zone become faster significantly as the molecular weight is decreasing towards M_e. Except for polystyrene, there are not sufficient results to indicate clearly the onset and the magnitude of the molecular-weight dependence of the transition zone for different polymers. With the frictional factor K for polystyrene being independent of molecular weight as guidance for the universal behaviour in the plateau-terminal region, the molecular-weight dependence in the transition zone should not be used directly as the basis for the iso-frictional correction for the study of the molecular-weight dependence of viscosity,[47] which is dominated by the K-determined long-time relaxation processes. Furthermore, as the temperature dependence in the glassy-relaxation region or the transition zone

has been shown to be stronger, as in the polystyrene case under the present study, than in the rubber-fluid range for several different polymers,[36,48,49,50,51] the temperature dependence in the transition zone should not be used directly for correlating viscosity data measured at different temperatures as one of the involved temperatures is sufficiently close to T_g.[44]

4.4. Basic Mechanism for the Thermorheological Complexity. The process $A_G\mu_G(t)$ that describes the $J(t)$ curve in the small-compliance/short-time region is clearly derived from energetic interactions among segments. As shown above, the chain section of the Rouse-segment size is gradually stiffened by the energetic interactions with decreasing temperature until it is overwhelmed by the effect at $\sim T_g$. Correspondingly, the increase in the parameter s with decreasing temperature suggests the existence of an additional dynamic time scale "normalised" with respect to K, which in turn suggests the existence of a corresponding structural length scale. Indeed, as s has the unit of $(\mathrm{Da})^2$, the mass size of the structure increases as $\propto s^{1/2}$ with temperature decreasing toward T_g. Clearly, such a structure has to be based on energetic interactions among segments. Based on what we have observed in the above analysis, this structure should have the following basic properties:

(1) The structure has a length scale and a lifetime, both of which increase with decreasing temperature. We can somewhat arbitrarily choose G/R=3 as a criterion for designating the lifetime of the structure. G/R=3 indicates a state which has relaxed considerably from $G/R\sim$10–by a factor of $\sim e^{-1}$–which is about the value at $t=\tau_A{}^{15}$ when the temperature is at T_g; at the same time, the state is still much under the influence of the energetic interactions. Thus, the time when G/R reaches 3 can be regarded as a time constant that reflects the duration of the structure. Here, we simply refer to it as the lifetime of the structure and denote it by τ_S. From the calculations whose results are shown in Figures 5 and 6, one finds that for both the samples while $\tau_S < \tau_A{}^{15}$ at ~104.5-105.5°C, τ_S has reached $\tau_A{}^6 \sim \tau_A{}^7$ at $\sim T_g$. $\tau_A{}^p$ is the relaxation time of the mode of motion associated with a length scale $\sim (a^2/p)^{0.5}$ where a is the entanglement distance.[5,52] Thus, the size of the domain influenced by the energetic interactions increases as

the temperature is lowered towards T_g. Of course, this is directly corresponding to the increase in the mass size of the structure ($\propto s^{1/2}$) as pointed out above. As defined above, the structural lifetime τ_S is of the order of $15\sim20\langle\tau\rangle_G$. And the length scale affected by the glassy-relaxation process or the length scale of the structure is ~ 3 nm (for p=6~7; and a=7.6 nm for polystyrene[5,38,53]) at ~ T_g. Interestingly, this length-scale value for polystyrene is the same as that estimated from the calorimetric data based on an argument considering fluctuations in a 'cooperatively rearranging region.[54,55] In general the length scales of glass-forming materials as obtained by different techniques are in the range 1~5nm.[54,55,56,57,58] The crossing over $\tau_A{}^{15}$ by τ_S just before the temperature reaches T_g is a critical microscopic event for the eventual vitrification of the polymer material. In the accompanying paper,[31] for being able to reflect the temperature dependence of the glassy-relaxation process accurately and the effect on bulk mechanical property by maintaining the same order of magnitude, the structural relaxation time is defined as $\tau_S=18\langle\tau\rangle_G$ (see Table 2); the relative changes of these two kinds of characteristic times with temperature in the case of sample A will be further studied.

(2) As induced by an applied strain, the stress on such a structure is developed on energetic interactions, and relaxes as the interlocking of segments in the structure loosens up due to thermal motions. The structural lifetime is an important factor that needs to be included in the consideration of the diffusion constant associated with a Rouse segment, D, when the structure has a size greater than that of the Rouse segment as described above. Even when the length scale of the structure is greater than that of the Rouse segment, D can still be defined by the distance a Rouse segment has travelled statistically over a *long period of time*. This is clear as, in the rubberlike-fluid region, the $J(t)$ line shape remains unchanged with temperature;[59] the relaxation times: $\tau_A{}^1$, τ_X, τ_B and τ_C, which are inversely proportional to D,[2,5-8] can be calculated from the K value obtained from the line-shape analysis as explained in Section 3.2. In other words, as K can be determined–as listed in Table 1 of ref. 31 for sample A from 127.5 to 97°C–so D can be defined and obtained.

Based on the basic properties of the structure as described above, the thermorheological complexity between the glassy-relaxation region and the rubber-fluid region can be explained as in the following: Being Brownian motion, the diffusion constant of a Rouse segment can generally be expressed as

$$D = \frac{kT}{\zeta} \approx \frac{l^2}{\Delta t} \qquad (9)$$

where l is the step length that the Rouse segment has moved in a time interval Δt. The only criterion for choosing Δt and l is that the steps are *independent* of one another; after a sufficiently large number of steps of movement have taken place, the central limit theorem assures that the dynamic process becomes Gaussian.[5,52] Here, we consider the time step Δt in a "normalized" scale by dividing it by K. The normalization has a similar sense as Figures 1, 2, 5 and 6 being displayed under a fixed K. As what will be discussed below has much to do with the fact that the normalized glassy-relaxation time s increases with decreasing temperature, it will be easier to explain the concepts in the normalized time scale. In the normalized scale, D is a constant–independent of temperature. When there is not the structure whose relaxation is described as above–as the situation expected to be at high temperatures–we can have a wide range down to very small values to choose l and Δt for satisfying eq 9. This is often referred to as the continuous (small-step) or "free" diffusion.[39,60] At a temperature close to T_g, the structure is formed with a certain lifetime τ_S (in the normalized scale), which increases as s increases; then the smallest independent time step that can be chosen is of the order of the lifetime of the structure $\Delta\tau \approx \tau_S \approx 15\sim 20\langle\tau\rangle_G$ (all in the normalized scale). We can choose $\Delta\tau$ as the time step because $\Delta\tau$ is still much shorter than τ_A^1, τ_X, τ_B and τ_C (all these time constants are constant in the normalized scale). Here, what has changed is that the diffusion regime has moved to longer

times. Corresponding to $\Delta\tau$ being longer, a larger length scale d is expected for the step length. And both $\Delta\tau$ and d increase with decreasing temperature. With $\Delta\tau$ and d chosen this way, the *normalized* diffusion constant can be kept constant as required. Because of the formation of the structure, the local segmental reorientation time directly related to the lifetime of the structure has lengthened greatly in the normalized time scale; however, the relaxation times (normalized) in the long-time region: $\tau_A{}^1$, τ_X, τ_B and τ_C, remain the same. In other words, in the real time (not normalized), the relaxation times in the long-time region are proportional to $K \propto \zeta/kT \approx \Delta\tau/d^2$ when the structure is formed, while the local structural relaxation time is proportional to $\langle\tau\rangle_G \propto \Delta\tau$. The temperature dependence of $\Delta\tau$ is expected to be stronger than that of $\Delta\tau/d^2$. This difference in temperature dependence is the basic mechanism for the thermorheological complexity as indicated by the analyses of the $J(t)$ curves at different temperatures in this study.

To satisfy the conditions for choosing $\Delta\tau$ and d, a likely dynamic process for the Rouse segment to take is by cooperative large-step jumping involving more than one Rouse segment. The cooperative large-step jumping has long been recognized based on the magnitude of the apparent activation energy near the glass transition.[39,61,62] Molecular dynamic simulations for glass-forming Lennard–Jones mixtures,[60,63] through the study of the van Hove self-correlation function, have clearly indicated the shifting of the diffusion regime to longer times as the temperature is lowered–similar to the effect as pointed out in the above analysis. Associated with this effect taking place is that the dynamics become not only spatially heterogeneous but also dynamically correlated; in other words, the dynamic process is no longer that described by continuous diffusion. Such dynamic heterogeneity and correlation have also been observed directly by confocal microscopy in the colloidal fluids near T_g.[64] Dynamic heterogeneity in glass-forming liquids and polymers in the vicinity of T_g has also been indicated by various studies using different techniques.[65,66,67,68,69,70] It is generally believed that dynamic heterogeneity implies the existence of a length scale, whose value at T_g, as much stimulated by the notion of the cooperative rearranging regions (CRRs) of the Adam and Gibbs theory,[71] has

been a subject of both theoretical and experimental studies.[54-58,72] In spite of all the gained understandings, a precise relation between the length scale or CRRs and dynamic heterogeneity has still to be formulated. The time scale and the length scale involved in the above discussion of the thermorheological complexity are obtained from analyzing the bulk property $J(t)$; thus, they are macroscopically averaged values. How these values can be better defined at the molecular level should be most likely answered by comparing studies with various spectroscopies.

The viscoelastic behaviour of polystyrene in approaching T_g as discussed above–namely, the discussion of $\langle\tau\rangle_G$ or τ_S vs. τ_A^1, τ_X, τ_B and τ_C–demonstrates what has been well said by Sillescu[54] about a dynamically heterogeneous system: "--, a system may be heterogeneous and non-ergodic at times t <1 s, but perfectly homogeneous and ergodic on a time scale of hours." To further illustrate this, we can use the K and s values for sample A approaching T_g as listed in Table 1 of the accompanying paper[31] to calculate the nonergodic and ergodic relaxation times for comparison as shown in Table 2. In the relatively short yet macroscopic time scales of $\langle\tau\rangle_G$ or τ_S, the strong energetic interactions in forming the structure keeps many configurations from being explored, while in the long time scales of τ_A^1, τ_X, τ_B and τ_C, there are enough time to explore the configurational space effectively, leading to entropy-derived modulus (as represented by the entropy force constant) and dynamics (as described by the Langevin equation). Below ~110^{o}C, loss of ergodicity gradually takes effect in polystyrene.

The formation of an energetic interactions-based structure indicates that the glass transition is a thermodynamic phenomenon; at the same time, the structure having a lifetime indicates that it is also a dynamic phenomenon. The dual nature of the glass transition phenomenon has long been recognized experimentally. For a practical purpose, a T_g-related temperature is often determined by monitoring the occurrence of the glass-rubber relaxation by dynamic mechanical measurements fixed at a certain frequency as the temperature is varied.[1,73] Since both K and s change with temperature, so does the characteristic time of the glass-rubber

relaxation in $G(t)$–often referred to as the α-relaxation time. Thus, the T_g-related temperature determined this way depends on the probing frequency. The traditional ways of defining the α-relaxation time will be compared with what will be obtained from the further analysis in the accompanying paper.[31] Another factor: non-equilibrium state at and below T_g, makes the measured T_g depend on the cooling rate of the sample. Such an effect can be clearly observed in monitoring the specific volume as the temperature is lowered.[1,74] In this study, the non-equilibrium aspect of T_g is not a concern, as the systems under analysis should all be in the equilibrium state.[19] Either probing rate or cooling rate is an externally imposed condition. In this report, we show that there is an intrinsic rate or time scale that plays a critically important role in the glass transition of a polymer, namely the relaxation time of the highest Rouse–Mooney mode, τ_A^{15}. The crossing over τ_A^{15} by τ_S signals the start of vitrification at the Rouse-segmental level–the basic change at the molecular level corresponding to the transition of the bulk consistency from rubber to glass. Since the Rouse segment is the most basic structural unit in terms of which all the long-time viscoelastic behaviour of the polymer can be described,[5] a fundamental change at the Rouse-segmental level–vitrification–is expected to have a dramatic effect on the bulk property. As the relative position of τ_S to τ_A^{15} is changed by the thermorheological-complexity effect, the glass transition is closely related to the observed thermorheological complexity in $J(t)$. This topic will be further studied in the accompanying paper.[31]

Models have been proposed for the supercooled liquids involving the concept of domain,[39,71,75,76,77] all based on energetic interactions among particles or segments. A basic idea in all these is, either explicitly or implicitly, that the system moves from the region of free diffusion to one of "landscape"(potential-energy hypersurface)-dominated dynamics as the temperature decreases towards T_g. Such a view is much supported by molecular dynamics simulations.[78,79] However, the thermorheological complexity–arising also from energetic interactions and related to the glass transition by the above-described mechanism–has never been

considered in any of these models, as far as we know. The temperature dependence of K is usually described by the Fulcher and Tammann–Hesse (FTH) equation or the Williams–Landel–Ferry (WLF) equation.[1,80,81] The thermorheological complexity is more than the non-Arrehnius temperature dependence, which has been provided an explanation for or accepted in these models.

Similar to the phrase "vitrification at the Rouse-segmental level" used to represent the overwhelming of the entropy-derived modulus by the energetic interactions-derived contribution at the Rouse-segmental time scale $t=\tau_A$[15] as revealed above, Adachi and Hirano[51] proposed an idea of local vitrification based on their observation that below 230K the ratio of the relaxation times of the normal and segmental modes in poly(*cis*-isoprene) as observed by dielectric relaxation decreases with decreasing temperature. However, their physical picture is totally different; they attributed the weaker temperature dependence of the normal mode to the shortening of the effective normal-mode length scale caused by the vitrification taking place locally at some points distributed on the chain. They also reported that they did not observe the decrease in the relaxation strength $\Delta\epsilon$ and broadening of the distribution of the normal-mode relaxation times to support their picture. Although not really a direct indication of local vitrification as shown in the present analysis, their observation that the time-temperature superposition is not applicable over the whole frequency range as the temperature approaches T_g should arise from the same basic mechanism as for the thermorheological complexity in $J(t)$ of the polystyrene system under the present analysis, just as the stronger temperature dependence of the glassy component in comparison with that of the rubbery component as revealed by Inoue *et al.* analyzing the dynamic mechanical and birefringence results for several different polymers.[12,13,49,50] Thus, the thermorheological complexity is quite a general phenomenon; the existence of such an effect has been pointed out by the researchers in polymer rheology through the years without offering a fundamental explanation.[12,13,36,48,49,50] In this study, we show through the analysis and discussion of $\langle\tau\rangle_G$ or τ_S vs. τ_A[1], τ_X, τ_B and τ_C the mechanism behind it

and its relation to the glass transition of a polymer.

The basic mechanism as proposed for the thermorheological complexity occurring in the polystyrene system should also be the reason for the breakdown of the Stoke–Einstein equation in relating the translational diffusion constant D_g with the shear viscosity η_s, which has been observed for glass-forming liquids, such as OTP (o-Terphenyl) [82,83,84] and TNB (tris-Naphthylbenzene),[85] when T_g is approached from above. Without the entropy-derived modes of motion as described by ERT in such liquids, $\eta_s \sim \int A_G \mu_G(t)\, dt$; similarly to what is explained above, $D_g \sim d^2/\Delta\tau$ while $\eta_s \sim \Delta\tau$. Thus, the diffusion constant is enhanced.

4.5. Free Volume and Relaxation Times. The frictional factor is responsible for the temperature dependence of the relaxation times, mainly following the FTH or WLF equation. Thus, according the traditional idea, the frictional factor is related to T_g in a certain way. It has been well known that free volume is a useful concept for describing the molecular-weight dependence of T_g [1,42, 86] and the steep increase of viscosity with temperature decreasing towards T_g.[1,87] In other words, the free volume in a polymer depends on temperature as well as molecular weight. The molecular-weight dependence of the free volume is mainly associated with the number of chain ends per unit volume. While K is shown independent of molecular weight, T_g has changed by about 8 degrees for polystyrene over the studied molecular-weight range ($\geq M_e$).[42,43] The explanation for this seemingly unusual phenomenon is that K is associated with the modes of motion along the primitive chain: $\mu_X(t)$, $\mu_B(t)$ and $\mu_C(t)$, to which the free volume localized at both ends of the chain is always available. Such a mechanism is very similar to the behaviour of clusters of mobile particles found in the molecular-dynamics simulation of a glass-forming Lennard–Jones liquid and observed in a supercooled colloidal fluid.[88] On the other hand, K' being associated with the $\mu_A(t)$ process–the normal modes of motion of an entanglement strand with *both ends fixed*–is affected by the average free volume in the neighbourhood of the whole entanglement strand, which is a function of the molecular weight of the bulk. As a result,

K''/K decreases with decreasing molecular weight (eq 8). The comparison of the results of the two studied samples indicates that s, while increasing with decreasing temperature, has the same molecular-weight dependence as that of K'/K over the shown temperature range (Figure 3). Similarly to K', T_g depends on molecular weight for being related to the free volume of the bulk polymer, which increases with the number of chain ends per unit volume. It is interesting to note that for polystyrene K' and T_g start to decline with decreasing molecular weight from a plateau value at about the same molecular weight ~$10M_e$.[43] The dynamic anisotropy as represented by $K''/K>1$ disappears—i.e. $K''/K \to 1$—as M decreases toward M_e. Thus, the molecular-weight dependence of K''/K as well as s should be related to entanglement, though in an indirect or "feedback" way, as entanglement has a length scale larger than those associated with the motions involving K' and s. In the above discussions, we show that the molecular-weight dependence of T_g should be only related to the $\mu_A(t)$ and $\mu_G(t)$ processes, whose relaxation times depend on molecular weight as K'. On the other hand, the relaxation times of the $\mu_X(t)$, $\mu_B(t)$ and $\mu_C(t)$ processes depend on molecular weight through their structural factors; their frictional factor K is independent of molecular weight.

What we have obtained here and previously suggest that some of the traditional views need be re-examined and refined regarding polymer viscoelasticity and glass transition. For further studies, the key observations are summarized as in the following:

(1) The frictional factor K is independent of molecular weight to as low as just above M_e; the change in K with temperature is entirely responsible for the temperature dependence of the relaxation times: τ_X, τ_B and τ_C.

(2) The ratio of K''/K exhibits the normalized-molecular-weight dependence as described by eq 8.

(3) K and K' are for the dynamic processes with a relaxation strength or modulus derived from entropy, i.e. without involving a structure based on energetic interactions. Thus, K

and K' should depend on temperature in the same way. The validity of this reasoning is supported by the result that the change in the $J(t)$ line shape with temperature is uniquely and fully described by the simple change in $s=\langle\tau\rangle_G/K$ as well as confirmed by the result obtained by Inoue *et al*.[12,13]

(4) The parameter s depends on temperature and molecular weight as shown in Figure 3. The mass size of the energetic interactions-based structure formed in approaching T_g is proportional to $s^{1/2}$. From 115~120°C to ~ T_g, the mass size of the structure has increased by a factor of ~3 for both the samples.

(5) In spite of the small distortion in the $A_G\mu_G(t)$ line shape of sample B by the residual plasticizers it contains, the result of analysis indicates that s between the two studied samples over the shown temperature range has the same molecular-weight dependence as K'/K; in other words, the dynamics in the whole $\mu_G(t)$-$\mu_A(t)$ region, not limited to the $\mu_A(t)$ process, are characterized by relaxation times maintaining the molecular-weight dependence same as that of K'/K given by eq 8. The ratio of s between the two studied samples at the same temperature should not mean that the mass size of the structure is greater in sample B than in sample A. The molecular-weight dependence of s following that of K'/K should arise from the same effect that is responsible for the molecular-weight dependence of K'/K, which is attributed to the free-volume effect associated with the number of chain ends per unit volume.

In the above list, points (1) and (2) are the results of the previous studies; points (3), (4) and (5) are based on the present study. In view of the universal nature of viscoelastic behaviour in the plateau-terminal region, point (1) should be universal. The temperature-dependence trend as given in point (4) is well supported by studies of polymers other than polystyrene showing that the temperature dependence in the glassy-relaxation region or the transition zone is stronger than in the rubber-fluid range, as pointed out in Section 4.3. Also pointed out in the same section, the

literature data in the glassy-relaxation region or the transition zone of other polymers indicate that the relaxation processes in the transition region become faster significantly as the molecular weight is decreasing towards M_e. This trend of change is the same as that of K'/K as given in points (2) and (5). However, whether the onset point of the decrease in the counter part of s or K'/K with decreasing molecular weight and magnitude of the molecular-weight dependence for other polymers will be as given by eq 8 remains to be seen. On the other hand, the limiting behaviour $K'/K \to 1$ as $M \to M_e$ should be universal.

The combination of point (1) and points (4) - (5) represents a quite different view from what has been held traditionally.[1] The fact that K being independent of molecular weight is rigorously proven by the results as shown in Table 1 strongly suggests that this view be valid. Thus, further studies in this area may lead to a totally new understanding of the glass transition phenomenon and its related dynamics.

5. Summary

Although the $J(t)$ results of Plazek of two nearly monodisperse polystyrene samples in the entanglement region were published more than 35 years ago, they remain basically unanalyzed, particularly in terms of a functional form which has a valid molecular theory as the basis. As a result, in spite of the extremely wide range of time they span, the rich information of polymer dynamics that they contain have remained basically untapped until this report.

In this study, two classes of contributions to the relaxation modulus $G(t)$ are identified: One, $A_G\mu_G(t)$, originates from energetic interactions; the other, containing the four dynamic processes of ERT: $\mu_A(t)$, $\mu_X(t)$, $\mu_B(t)$ and $\mu_C(t)$, is derived from entropy. The relaxation functional forms of all the processes are given: phenomenological form for $A_G\mu_G(t)$; molecular expressions for $\mu_A(t)$, $\mu_X(t)$, $\mu_B(t)$ and $\mu_C(t)$. In terms of the $G(t)$ function, the $J(t)$ results of Plazek are successfully analyzed. We first show that the $J(t)$ results of the two nearly monodisperse polystyrene samples are well described by ERT in the rubber(like)-fluid region,

giving the frictional factor K for the uncontaminated sample–sample A–in quantitative agreement with those obtained previously from analysing the $G(t)$ results and calculated from the viscosity and diffusion data. This gives an confirmation–from an independent investigator and different type of measurement–to the validity of ERT. Then it is demonstrated that the successful description of $J(t)$ in the rubber(like)-fluid region in terms of ERT can be used as the reference frame, with respect to which the glassy-relaxation process that occurs in the small-compliance/short-time region of $J(t)$ can be analysed meaningfully and profitably. The contributions from this study are manifold:

The unified quantitative analysis of the whole range of chain dynamics, from the glassy-relaxation region to the flow region, shows how the dynamic processes occur one after another as clearly displayed in the $G(t)$ form. Displaying the hierarchy of the dynamic processes in perspective, the analysis by itself has far-reaching application potential, for instance, for comparing studies with other spectroscopies sensitive to dynamics at different length scales and for seeing how the hierarchy is affected if some structural modification is made to the polymer.

It is shown that in polystyrene the temperature dependence of the energetic interactions-derived glassy-relaxation process is stronger than that of the entropy-derived processes in the rubber-fluid region as the temperature is close to T_g, in agreement with the result obtained by Inoue *et al*.[12,13] The thermorheological complexity in $J(t)$ is shown arising from this difference in temperature dependence; the temporal unevenness in the observed complexity in $J(t)$ is revealed as due to the smearing effect of the convolution integral in eq 3.

Corresponding to the thermorheological complexity, the increase of the normalized glassy-relaxation time s with decreasing temperature indicates that a structure based on energetic interactions among segments occurs as the temperature is close to T_g. With decreasing temperature, both the length scale and lifetime of the structure increase; furthermore, the mass size of the structure is expected to increase as $\propto s^{1/2}$.

This study, making use of the molecular picture in ERT, gives microscopic information

about the glass transition of polystyrene from a viewpoint that cannot be reached by the traditional approaches.[39] In fact, the entanglement effect has often been seen as an "obstacle"–by causing a viscosity increase of many orders of magnitude–to the study of the glass transition of a polymer when the convention of viscosity reaching 10^{13} poise[39,40] is to be used to indicate T_g. Here, because ERT enables the whole rubber(like)-fluid region in $J(t)$ to be analyzed, we turn entanglement to our advantage–namely, using the description of rubber-fluid region as a reference frame for studying the glassy-relaxation process that occurs in the short-time region. Through the molecular picture of ERT, the following two important pieces of information related to the glass transition have been revealed: (a) It is shown that for polystyrene the length scale of the energetic interactions-based structure is ~3nm at T_g in agreement with the value obtained from the calorimetric data.[54,55] Much to the credit of the notion represented by the 'cooperatively rearranging regions' of the Adam and Gibbs theory, the length scale at T_g has been the focus of various studies. This study represents a new methodology for studying it in an entangled polymer. As opposed to several techniques which require imposing external length scales to the studied material,[54-58] the yardstick for estimating the length scale in this study is provided internally–i.e. by the normal modes in the $\mu_A(t)$ process. This method has the advantage of being free of any surface effect which may quite easily affect the result in the case that the material is studied in confined geometries; the surface effect is currently very much an issue of interpretation. In principle, the present method can be applied to any entangled polymer, as long as it is nearly monodisperse.[89,90] This would be particularly useful as the values of entanglement distance, a, of various polymers have been well documented.[5,38, 53] (b) It is shown that, corresponding to the rubber-glass transition of the polymer taking place at the calorimetric T_g, τ_S becomes greater than τ_A[15] indicating vitrification at the Rouse-segmental level. Such a fundamental change at the Rouse-segmental level should be responsible for the dramatic change in the bulk mechanical property at ~T_g. τ_S becoming greater than τ_A[15] at ~T_g for a polymer

suggests the question whether there is a physical time constant τ_l that can be studied, characterizing the liquid state in a glass-forming liquid, which is to be surpassed by the structural-(α-) relaxation time τ_S for the glass transition to take place. So far such a time is set in an arbitrary way by the convention that τ_S reaches 100~1000 s at ~T_g.[39,54,91] The τ_S value at ~T_g shown in Table 2 is consistent with the convention.

It is shown that the basic mechanism for the thermorheological complexity deduced from the present study should be also responsible for the breakdown of the Stoke–Einstein relation observed in glass-forming liquids, such as OTP and TNB, near the glass-liquid transition. While the thermorheological complexity has been puzzling to polymer rheologists for years, the break-down of the Stoke–Einstein relation has been actively studied in the past decade. The proposed mechanism allowing the two seemingly unrelated phenomena to be linked represents a new way to see and study the glass transition phenomenon.

Acknowledgement

This work is supported by the National Science Council (NSC 92-2113-M-009-027).

Appendix: Comparison of the *K* Values Obtained from *G*(*t*), *J*(*t*), Viscosity and Diffusion Data.

Here, with respect to the frictional factor *K*, we make a more thorough comparison with the literature data than in ref. 6, particularly taking the effect of the finite molecular-weight distribution of the nearly monodisperse samples on their viscosity values into account. The contributions of the $\mu_A(t)$ and $\mu_B(t)$ processes to the viscosity are negligible when the molecular weight is sufficiently high (>7M_e). Under such a situation, an analytical expression for the viscosity can be obtained in ERT (see eq 29 of ref. 8 or eq 9.24 of ref. 5). Using this equation, *K* can be calculated from the viscosity and density data. The results obtained by Plazek and

O'Rourke [29] for samples with M_w= .94x; 1.89x; and 6.0x10^5 are used in the calculations giving K=7.1x, 5.9x, and 7.7x10^{-9}, respectively, at 127.5^{o}C; and 3.2x, 2.4x, and 2.7x10^{-12}, respectively, at 174^{o}C. It has been shown that the viscosity of a nearly monodisperse sample is slightly larger than that of an ideally monodisperse one with the same (weight-average) molecular weight.[2,5,92] Being for ideal monodispersity, the analytical expression leads to a slightly larger K value as the experimental viscosity value is used in the calculation with the weight-average molecular weight being regarded as the molecular weight in the equation. The bulk of correction can be made to the obtained K value if the M_w/M_n value is known. While being not given, the M_w/M_n values of the three samples can be estimated from matching their measured steady-state compliance J_e^0 values[29] with those calculated from the linear viscoelastic equation, $J_e^0 = \int_0^\infty G(t)tdt \Big/ \left(\int_0^\infty G(t)dt \right)^2$, wherein the $G(t)$ is first calculated from convoluting eq 1 with the Schulz distribution using the polydispersity parameter Z as the only adjustable parameter. In this way, Z=23, 20, and 10 (correspondingly, M_w/M_n=1.04, 1.05, 1.1) are obtained for the three samples, respectively. These values are well within the range expected for a nearly monodiperse sample. Then the correction factors for K due to the finite molecular-weight distribution can be obtained by comparing the viscosity results calculated from the analytical equation and from integrating numerically the $G(t)$ which has first been calculated from convoluting eq 1 with the Schulz distribution using the above obtained Z values, both kinds of calculations being done with the same (weight-average) molecular weight and K for each sample. The thus obtained correction factors are 1.24, 1.22, and 1.34 for the three samples, respectively. That the first sample, while having a Z value slightly larger than the second one, has a slightly larger correction factor is due to the fact that at its molecular weight the $\mu_A(t)$ and $\mu_X(t)$ processes can still make a small noticeable contribution to the viscosity. Taking the correction factors into account, the K values are obtained to be 5.7x, 4.9x, and 5.8x10^{-9}, respectively at 127.5^{o}C; and 2.6x, 2.0x, and 2.0x10^{-12}, respectively at 174^{o}C.

In ref. 6, the diffusion proportional constant $K_d = D_G M^2$ determined directly by the

diffusion measurements and calculated from the frictional factor K ($K_d=\langle R^2\rangle M_e/3\pi^2 MK$) obtained from the analyses of the viscoelastic data are compared at 174°C. The comparison can be equivalently made in terms of K instead of K_d; see ref. 6 for the details. From the K_d value (8×10^{-3} cm^2(Da)^2/sec) of Kramer *et al.*,[33-35] one obtains $K=2.5\times10^{-12}$ at 174°C.

The above K values obtained at 127.5 and 174 °C along with those obtained from analysing the $G(t)$ and $J(t)$ results are listed in Table 1. The K values at 127.5°C as listed in the first row of the table represent the viscoelastic results of totally 11 samples of different molecular weights ranging from 3.4×10^4 to 6×10^5; the average over these samples with equal weighting is $4.9_3\times10^{-9}$ with a standard deviation of 10% which is basically the same statistically as the average listed in the first row. In the same series of samples whose $G(t)$ results were analyzed, a sample with a molecular weight just above M_e ($M_w=1.67\times10^4=1.24M_e$) gives $K=4.0\times10^{-9}$, which is about 20% lower than the above average value. Considering the fact that the molecular weight of this particular sample is so close to M_e and that any small amount of the components in its molecular-weight distribution having molecular weight smaller than M_e has the effect to reduce the obtained K value somewhat, this deviation, though greater than the standard deviation by a factor of ~2, is very consistent with the results of other samples. If this sample is included in the statistical analysis, the average is $4.8_5\times10^{-9}\pm11\%$. The results listed in Table 1 as well as discussed above clearly show that the K values obtained independently from different kinds of measurements: $G(t)$, $J(t)$, viscosity and diffusion are quantitatively consistent and that the constancy of K extends to the molecular weight as low as just above M_e.

Figure Captions:

Figure 1.

Creep compliance $J(t)$ data of sample A measured at 114.5 (▵); 109.6 (•); 104.5 (◦); 100.6 (▾); and 97 (▿) ^{o}C in comparison with the theoretical curves (—— ; from left to right, respectively) calculated with K=5x10^{-9}, G_N=1.89x10^{6} dyne/cm^{2}; and the A_G, β and s values as explained and given in the text.

Figure 2.

Creep compliance $J(t)$ data of sample B measured at 119.8 (▵); 113.8 (•); 105.5 (◦); 101.0 (▾); and 98.3 (▿) ^{o}C in comparison with the theoretical curves (—— ; from left to right, respectively) calculated with K=5x10^{-9}, G_N=1.89x10^{6} dyne/cm^{2} ; and the A_G, β and s values as explained and given in the text.

Figure 3

The normalized glassy-relaxation time s of samples A (◇) and B (○) at different temperatures. See the text.

Figure 4

Comparison of the $G(t)$ (——) and $J(t)^{-1}$ (•••) curves for sample B at 113.8 ^{o}C (same $J(t)$ as the corresponding one shown in Figure 2). Also shown are the curves calculated without the $A_G\mu_G(t)$ process: (– – –) for $G(t)$ and (◦◦◦) for $J(t)^{-1}$; the dotted line indicates the $G(t)$ curve calculated without both the $A_G\mu_G(t)$ and $\mu_A(t)$ processes.

Figure 5

Calculated $G(t)$ curves corresponding to three $J(t)$ curves shown in Figure 1 for sample A: a for

114.5°C (——), b for 104.5°C (– · –), and c for 97°C (– · · –). Line d is calculated without the $A_G\mu_G(t)$ process; line e is calculated without both the $A_G\mu_G(t)$ and $\mu_A(t)$ processes. The (– – –) lines from bottom up represent the sums of line e and the first 3, 6, 9, and 12 modes in $\mu_A(t)$, respectively. The dots represent the locations of the relaxation times as indicated. In the three dots under $\langle\tau\rangle_G$, the left one is for a; the middle one, for b; and the right one, for c.

Figure 6

Calculated $G(t)$ curves corresponding to three $J(t)$ curves shown in Figure 2 for sample B: a for 113.8°C (——), b for 105.5°C (– · –), and c for 98.3°C (– · · –). The rest are the same as in Figure 5.

TABLE 1: Frictional factor *K* from *G*(*t*), *J*(*t*), viscosity and diffusion results

	From $G(t)$ a series of samples[a] $3.4\text{x}10^4 \le M_w \le 1.1\text{x}10^5$	From $J(t)$[b] $M_w=4.69\text{x}10^4$	From Viscosity[c] $M_w=9.4\text{x}10^4$	$M_w=1.89\text{x}10^5$	$M_w=6.0\text{x}10^5$	From Diffusion[d]	Average[e]
$K(127.5^oC)\text{x}10^9$	4.7±8%	4.8	5.7	4.9	5.8	(5.7)[f]	5.2±10%
$K(174^oC)\text{x}10^{12}$	(2.1)[f]	(2.1)[f]	2.6	2.0	2.0	2.5	2.3±14%

[a] ref. 2.

[b] This study.

[c] ref. 29.

[d] refs.33–35.

[e] The average values are obtained from averaging over the values not enclosed in a bracket.

[f] Values in a bracket are calculated from the shown values at the other temperature using the ratio of the two average *K* values.

TABLE 2: Time Constants of Dynamic Processes in Sample A at Temperatures Close to T_g: Ergodic (Entropy-derived) vs. Nonergodic (or with Loss of Ergodicity; Energetic Interactions-derived)

Temp ^oC	With loss of ergodicity or nonergodic		Ergodic			
	$\langle\tau\rangle_G$ or sec.	τ_S	$\tau_A{}^1$	τ_X	τ_B	τ_C
			sec.			
104.5	.196	3.2 (3.53)[a]	587	4179	8798	19699
100.6	2.74	48.7 (49.4)[a]	4759	33779	71121	159232
$97 \approx T_g$	55.7	1193 (1002)[a]	48276	342661	721472	1615305

[a] Defined by $\tau_S = 18\langle\tau\rangle_G$; see ref. 31.

Figure 1

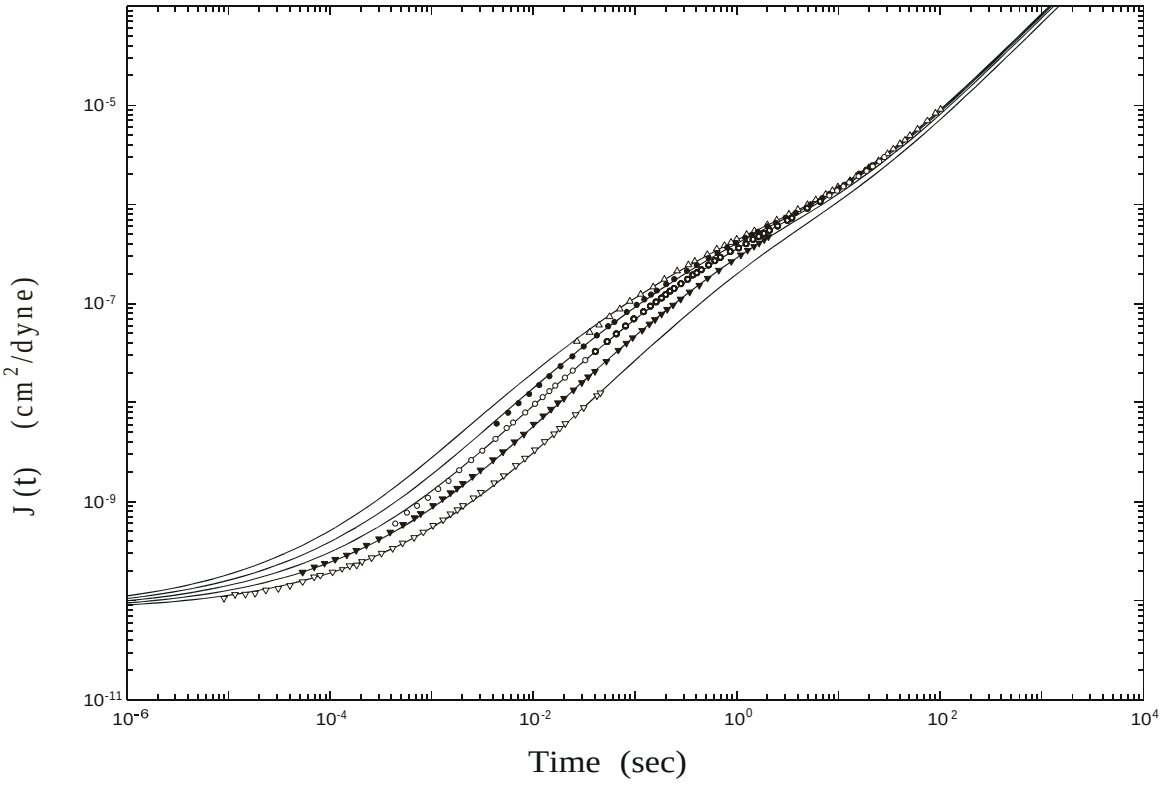

Figure 2

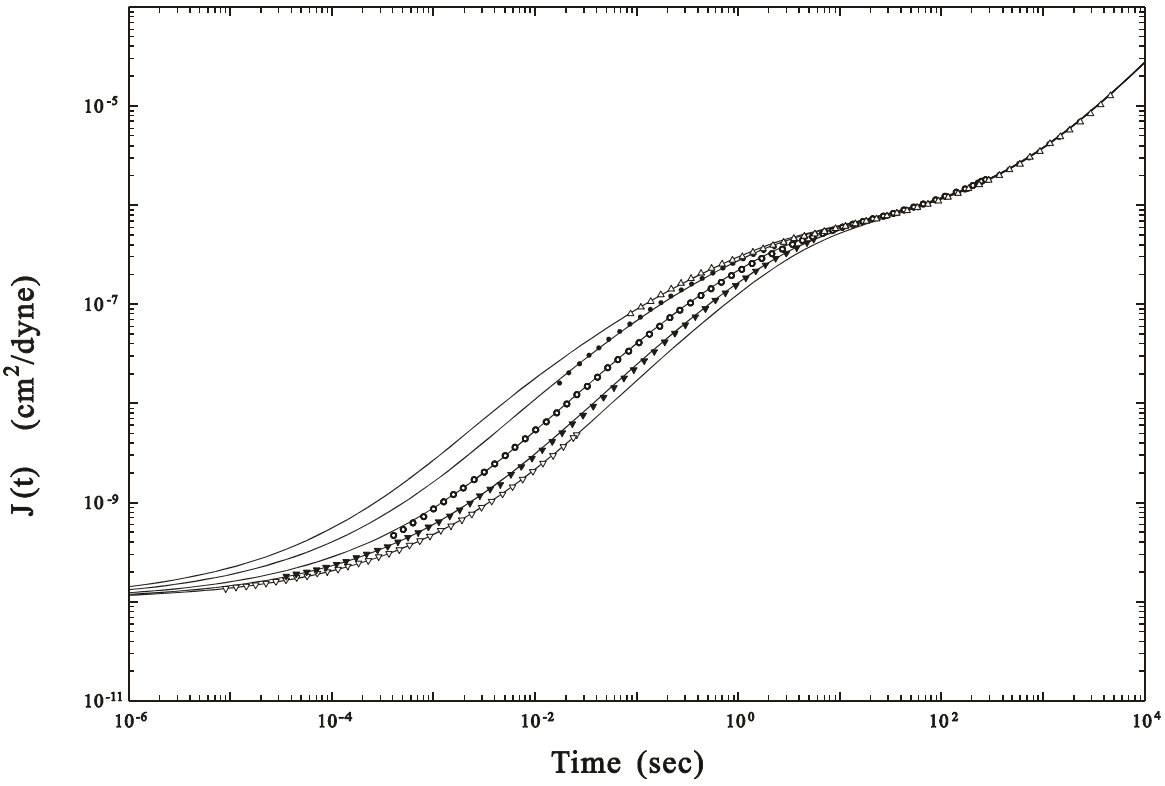

Figure 3

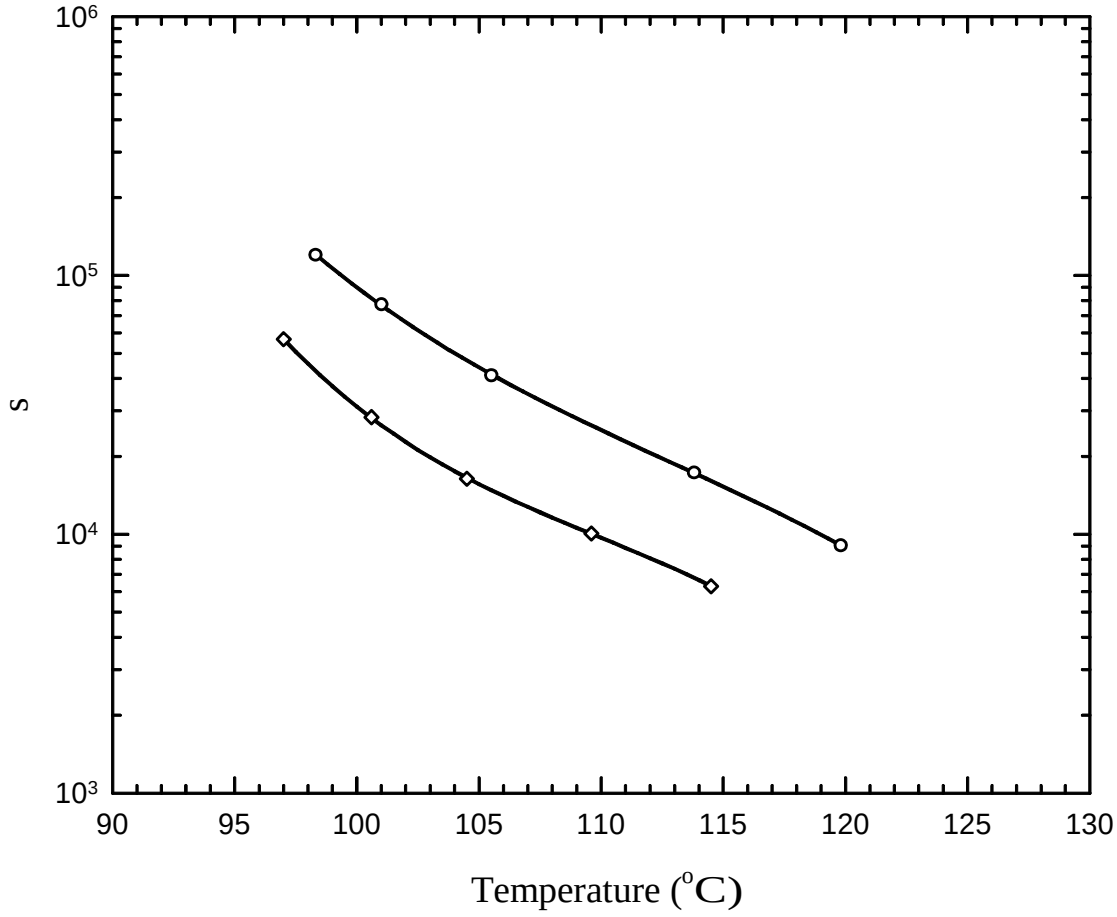
10^6
10^5
10^4
10^3
S
90
95
100
105
110
115
120
125
130
Temperature (°C)

Figure 4

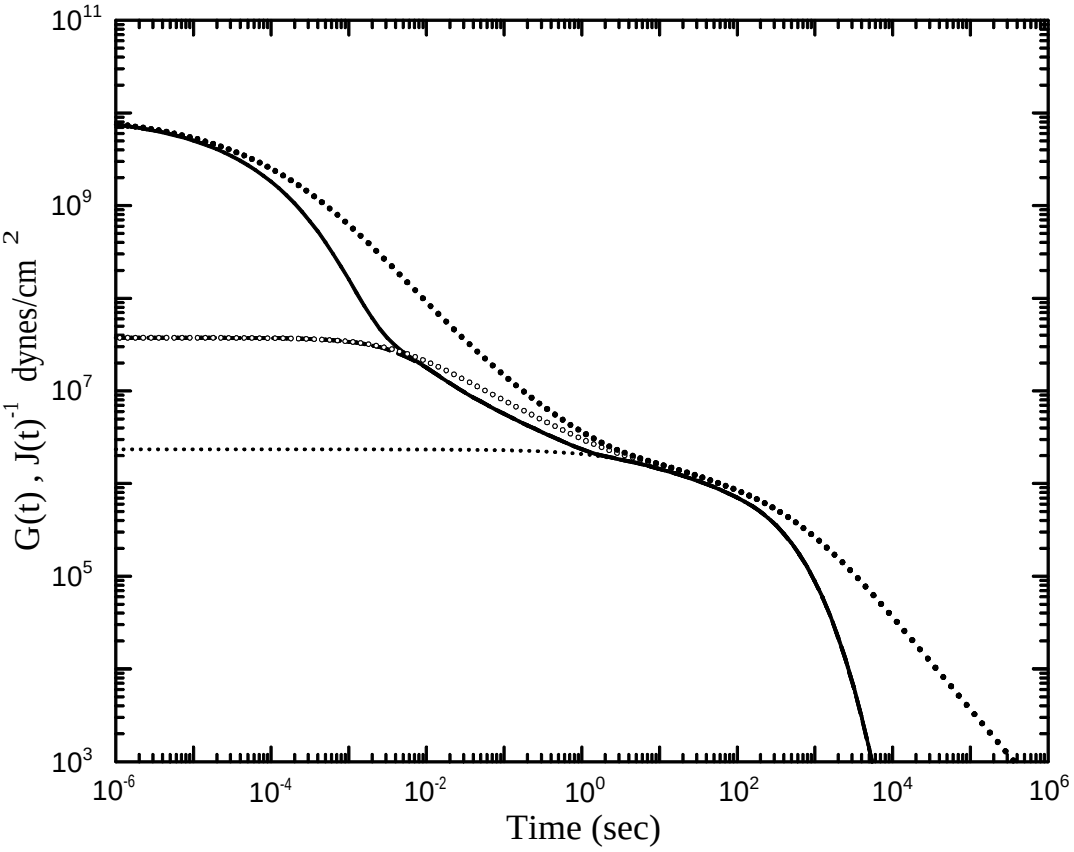
10^{11}
10^{9}
10^{7}
10^{5}
10^{3}
G(t) , J(t)$^{-1}$ dynes/cm ^{2}
10^{-6}
10^{-4}
10^{-2}
10^{0}
10^{2}
10^{4}
10^{6}
Time (sec)

Figure 5

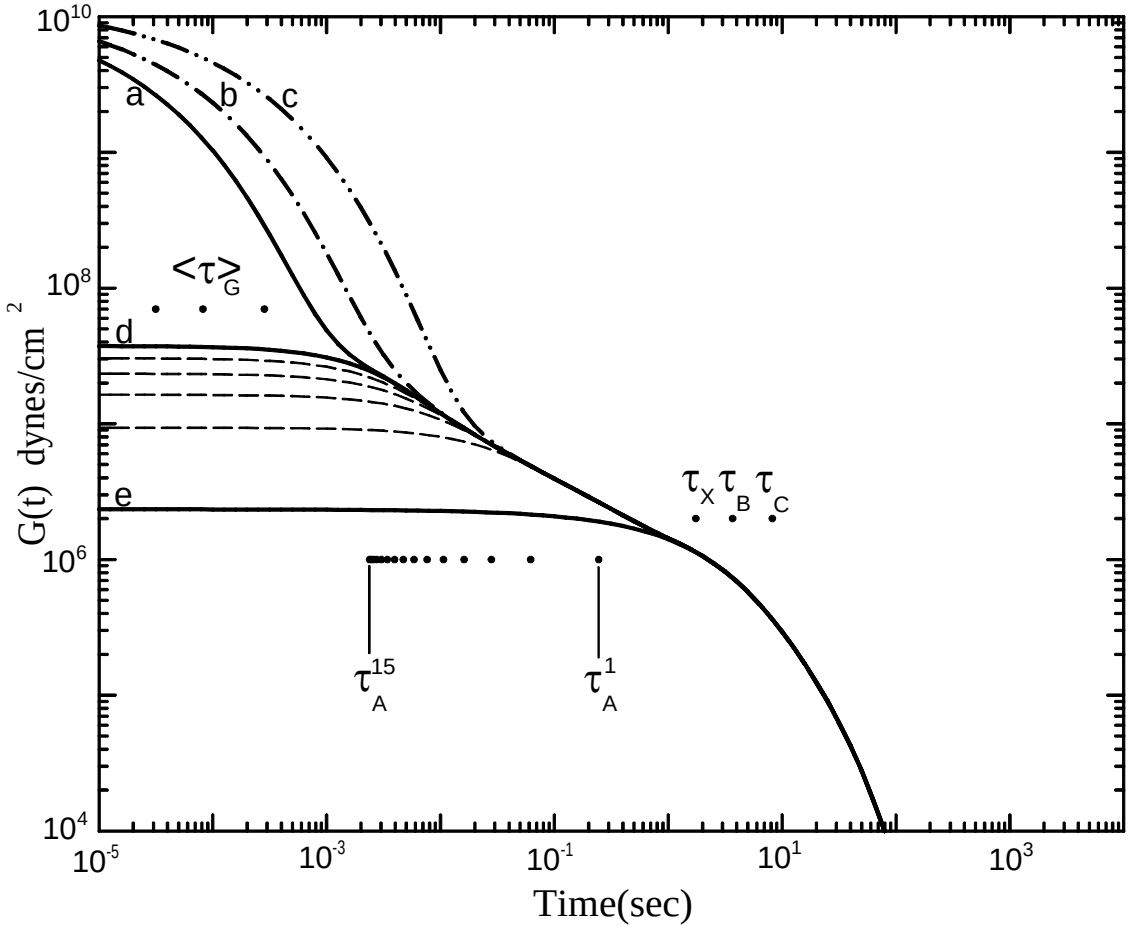
10^{10}
10^{8}
10^{6}
10^{4}
G(t) dynes/cm^2
a
b
c
d
e
$\langle\tau\rangle_G$
τ_X τ_B τ_C
τ_A^{15}
τ_A^{1}
10^{-5}
10^{-3}
10^{-1}
10^{1}
10^{3}
Time(sec)

Figure 6

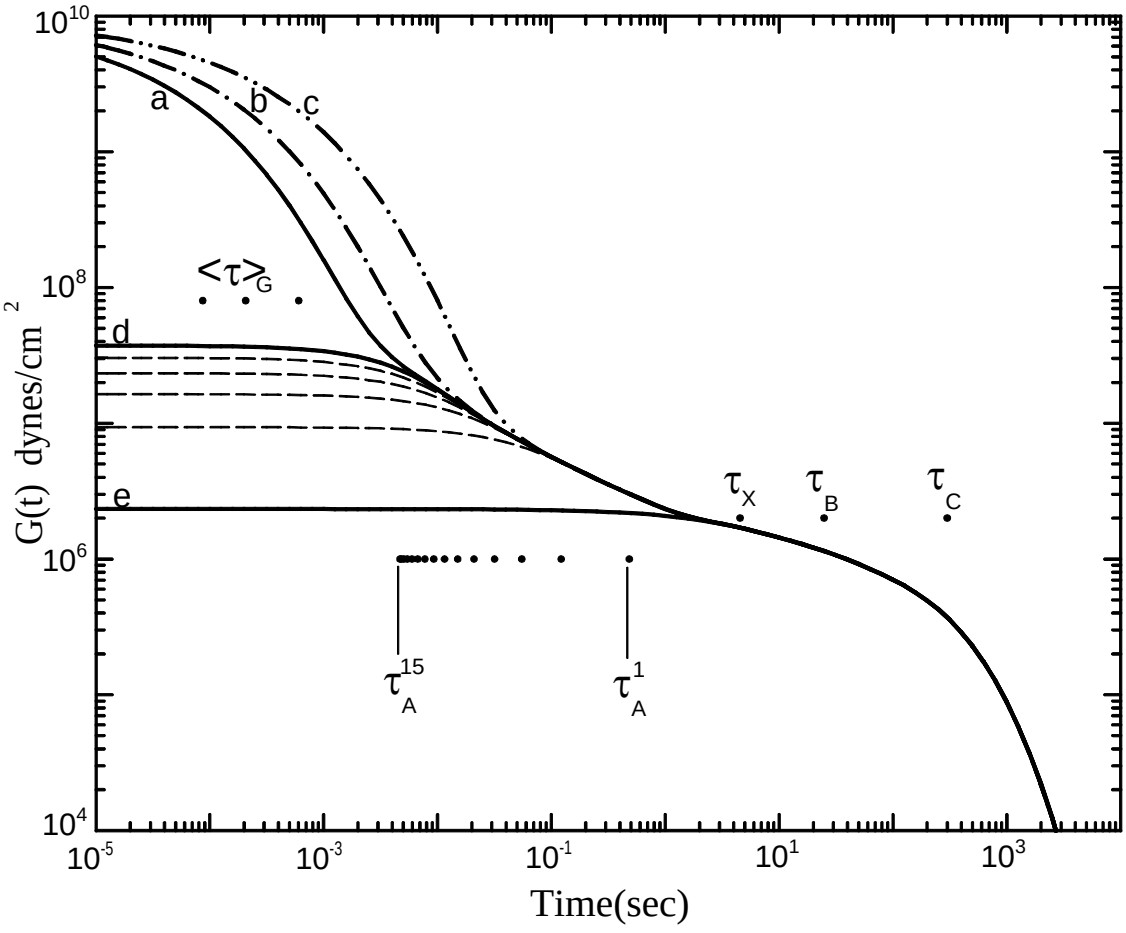
10^{10}
10^{8}
10^{6}
10^{4}
G(t) dynes/cm^2
a
b
c
d
e
$\langle\tau\rangle_G$
τ_X
τ_B
τ_C
τ_A^{15}
τ_A^{1}
10^{-5}
10^{-3}
10^{-1}
10^{1}
10^{3}
Time(sec)

Motion Associated with a Single Rouse Segment versus the α Relaxation

Y.-H. Lin[b]
Department of Applied Chemistry
National Chiao Tung University
Hsinchu, Taiwan

Abstract

The dynamics in polystyrene melt and concentrated solution as probed by depolarized photon-correlation spectroscopy has been shown to reflect the motion associated with a single Rouse segment. In the concentrated-solution case (entanglement-free), the analysis using the frictional factor K ($=\zeta\langle b^2\rangle/kT\pi^2m^2$) extracted from the viscosity data in terms of the Rouse theory and aided by the Monte Carlo simulation based on the Langevin equation of the Rouse model confirms the conclusion in a precise manner. In the melt case (entangled), the Rouse-segmental motion as observed by depolarized photon-correlation spectroscopy is compared with the α relaxation and the highest Rouse–Mooney normal mode extracted from analyzing the creep compliance $J(t)$ of sample A reported in the previous paper. Another well-justified way of defining the structural- (α-) relaxation time is shown basically physically equivalent to the one used previously. Based on the analysis, an optimum choice $\tau_S = 18\langle\tau\rangle_G$ ($\langle\tau\rangle_G$ being the average glassy-relaxation time) is made, reflecting both the temperature dependence of $\langle\tau\rangle_G$ and the effect

on the bulk mechanical property by the glassy-relaxation process. In terms of thus defined τ_S, two traditional ways of defining the α-relaxation time are compared and evaluated. It is shown that as the temperature approaches the calorimetric T_g, two *modes of temperature dependence* are followed by the dynamic quantities concerning this study: One includes the time constant of the highest Rouse–Mooney normal mode, τ_v; the temperature dependence of the viscosity corrected for the changes in density and temperature, $\eta/\rho T$; and the average correlation time obtained by depolarized photon-correlation spectroscopy, $\langle \tau_c \rangle$. The other, being steeper, is followed by the α-relaxation time τ_S derived from the glassy-relaxation process, and the temperature dependence of the recoverable compliance $J_r(t)$ as obtained by Plazek. The comparison of the dynamic quantities clearly differentiates the motion associated with a single Rouse segment as characterized by τ_v or $\langle \tau_c \rangle$ from the α relaxation as characterized by τ_S; due to the lack of clear definition of these two types of motion in the past and the proximity of one to the other in the time scale—actually the two crossing over each other—as the temperature is approaching T_g, the two modes could be easily confused. Below ~110°C, the rate of $\langle \tau_c \rangle$ changing with temperature lags behind that of τ_v is explained as due to the loss of effective ergodicity taking place in the system.

[b] E-mail:yhlin@mail.nctu.edu.tw

Motion Associated with a Single Rouse Segment versus the α Relaxation

Y.-H. Lin
Department of Applied Chemistry
National Chiao Tung University
Hsinchu, Taiwan

1. Introduction

The Rouse model[93] is based on picturing a polymer chain as a linkage of beads and springs.[94,95,96] Each bead-spring segment is often referred to as the Rouse segment. The distribution of the separation between two neighbouring beads is described by a Gaussian function. The motion associated with a single Rouse segment is basically equivalent to the highest Rouse normal mode of motion in a polymer chain. If the polymer chain is very long, and we are interested in only the few slowest modes of chain motion–for instance, as mainly reflected by the zero-shear viscosity–the length of chain section assigned to a Rouse segment is not an issue as long as the chosen section is much smaller than the whole chain and at the same time sufficiently long. However, the highest Rouse mode becomes relevant; and how to define a Rouse segment becomes a concern, if we are interested in the relatively fast T_g-related α relaxation which shows up in the high-modulus region of a typical viscoelastic spectrum as the temperature is lowered towards T_g.[97,98,99,100,101,102,103] An ideal Rouse segment cannot be found in reality, as the Gaussian function allows the spring between two beads to be stretched infinitely–a

situation that cannot occur because of the rigidity of chemical bonds. Thus, if a Rouse segment can be defined experimentally, it has to be probed in the linear region, for instance, by measurements of linear viscoelasticity and photon-correlation function. Furthermore, the Rouse segment as expected to be seen here is not a clear geometric identity but rather is represented by an optimum size or mass that, for instance in an entanglement-free case, allows the experimental results to be best described in terms of the *discrete* Rouse model for a chain with a *finite* number of beads.[3,4] In this report, the theoretical aspect of relating the depolarized photon correlation to viscoelasticiy in a concentrated polystyrene system will first be reviewed. Then, three related points will be addressed: (1) The dynamics in polystyrene melt and concentrated solution as probed by depolarized photon-correlation spectroscopy has been shown to reflect the motion associated with a single Rouse segment as expected from the theoretical analysis. In particular, it will be illustrated how this is shown in a precise manner in the entanglement-free concentrated solution case, supported by the agreement of the obtained mass of a single Rouse segment with that obtained by Inoue *et al*.[104] from analyzing the dynamic mechanical and birefringence results. The Rouse-segmental motion in melt (entangled) as observed this way will be compared with the α relaxation and the highest Rouse–Mooney normal mode extracted from analyzing the creep compliance $J(t)$ of sample A reported in the previous paper–the results of sample B cannot be used here because of its contamination by residual plasticizers. (2) A distinction between the Rouse-segmental motion as studied by the depolarized photon-correlation spectroscopy and the α relaxation should be made. Due to the lack of clear definition of these two types of motion in the past and the proximity of one to the other in the time scale, the mode of motion that should have been considered as the Rouse-segmental motion could be confused with the α relaxation.[105] (3) In this report, another well-justified definition of the structural- (α-) relaxation time is shown basically physically equivalent to the one used previously.[11] For reflecting both the temperature dependence of the glassy-relaxation process accurately and the effect on the bulk mechanical property, an optimum choice $\tau_S = 18\langle\tau\rangle_G$ is made. In terms of thus defined τ_S, two traditional

ways of defining the α-relaxation time[5] are compared and evaluated. Finally various dynamic quantities obtained from analyzing the depolarized photon-correlation and creep compliance results are compared and discussed.

2. A Summary of Molecular Theories of Polymer Viscoelasticity

Successful molecular theories of polymer viscoelasticity in the entanglement-free region–the Rouse model[4,106,107]–and in the entanglement region–the extended reptation model[4,108,109,110,111]– have been developed using the Rouse segment as the most basic–smallest–structural unit. These theories are mean-field theories; the bulk viscoelastic quantity is simply the sum of the average values from individual model molecules.[2-4] The friction constant ζ associated with each Rouse segment or equivalently the frictional factor K as defined below is a basic element of such a mean field: [4,11,14-19]

$$K = \frac{\zeta \left\langle b^2 \right\rangle}{kT\pi^2 m^2} \qquad (1)$$

where m and b are the mass and length of a Rouse segment, respectively. K alone carries the temperature dependence of the Rouse segment-based relaxation times, which often follows the FTH or WLF equation.[5] The extended reptation theory (ERT)[4,16] is developed by incorporating the intramolecular Rouse-type motions into the Doi–Edwards theory.[112] In addition to the use of the Rouse segment, ERT contains the basic mean-field assumption of the Doi–Edwards theory, i.e. the definition of the primitive chain as represented by the following equation

$$N\left(=\frac{M}{M_e}=\frac{N_o}{N_e}\right)=\frac{L}{a}=\frac{\left\langle R^2\right\rangle}{a^2}=\frac{N_o\left\langle b^2\right\rangle}{a^2} \qquad (2)$$

where L denotes the contour length of the primitive chain, a is the distance between two ends of an entanglement strand with mass M_e or equivalently N_e ($=M_e/m$) Rouse segments, and $\langle R^2 \rangle$ represents the mean square end-to-end distance of a polymer chain with mass M or equivalently N_o ($=M/m$) Rouse segments. The frictional factor K in ERT is shown to be independent of molecular weight to as low as just above the entanglement molecular weight M_e (see the Appendix and Table 1 of ref. 11), proving the validity of ERT.[4,14–19] The validity of the Rouse theory[4,14,15] as well as its consistency with ERT by sharing the same frictional factor K[4,18] has been extensively tested by experimental results. It is an important contribution of ERT to bridge the gap between the Rouse and Doi-Edwards theories by showing that they have the same footing at the Rouse-segmental level. Because of this result, the frictional factor K extracted from the viscoelastic results in terms of either the Rouse theory or ERT can be used in the same way in comparing with the depolarized photon-correlation results, as done previously[9,10,113,114,115] and in this study.

For both the studies of the motion associated with a single Rouse segment and the α relaxation, the strategy we take is to use the successful description of the slow (low-frequency) viscoelastic properties–for instance, the zero-shear viscosity and the viscoelastic spectrum from the low-frequency end of the transition zone to the terminal zone–in terms of the molecular theories as the reference frame.[9-11,21-23] The molecular theory used for analysing the experimental results depends on whether the system is in the entanglement or entanglement-free region. Then, the frictional factor K thus determined can be used to calculate the time constant of the highest Rouse normal mode for comparison with other dynamic results or be used to "normalize" the α-relaxation time for further comparative analysis.

In the Rouse model, the relaxation modulus $G(t)$ for a monodisperse polymer of molecular weight M or N_r beads is obtained as[1,3,4]

$$G(t) = \left(\frac{\rho RT}{M} \right) \mu_R (t / \tau_R) \qquad (3)$$

with

$$\mu_R (t / \tau_R) = \sum_{p=1}^{N_r - 1} \exp\left(\frac{-t}{\tau_R} \right) \qquad (4)$$

where ρ is the concentration of the polymer (mass per unit volume) and $\{\tau_R^p\}$ is given by

$$\tau_R^p = \frac{\zeta \left\langle b^2 \right\rangle}{24kT \sin^2\left(p\pi / 2N_r \right)} = \frac{K\pi^2 M^2}{24 N_r^2 \sin^2\left(p\pi / 2N_r \right)}; \qquad p = 1,2,... \ N_r - 1 \qquad (5)$$

For N_r>>1, the zero-shear viscosity may be obtained from $G(t)$ as

$$\eta = \int_0^\infty G(t) dt = K \left(\frac{\rho RT \pi^2}{36} \right) M \qquad (6)$$

If the molecular weight of a Rouse segment, m, is known, the relaxation time of the highest Rouse viscoelastic normal mode, τ_v, can be calculated according to

$$\tau_v = \frac{K\pi^2 m^2}{24} \qquad (7)$$

which is obtained by substituting $p=N_r-1$ into eq 5 and taking $(N_r-1)/N_r\approx 1$ for N_r sufficiently large. The frictional factor in eq 7 can be obtained from the viscosity data analysed in terms of eq 6. Thus, from the viscosity measurement, the information of the Rouse-segmental motion characterized by τ_v can be obtained.

A summary of ERT has been given in the previous paper[11] (eqs 1 and 2). The relaxation times of the $\mu_A(t)$, $\mu_X(t)$, $\mu_B(t)$, and $\mu_C(t)$ processes are each expressed as a product of the frictional factor K (denoted by K' for $\mu_A(t)$) and a structural factor. Except for the $\mu_A(t)$ process, we refer all the functional forms of the relaxation processes and their respective characteristic (relaxation) times to the previous publications.[4,16-18] As first shown by Mooney,[4,16,116,117] $\mu_A(t/\tau_A)$ and $\tau_A{}^p$ have the same forms as $\mu_R(t/\tau_R)$ and $\tau_R{}^p$ (eqs 4 and 5), respectively, with M replaced by M_e and N_r replaced by N_e. In applying the eq for $\tau_A{}^p$, the frictional factor K needs to be replaced by K' as given by eq 8 of ref. 11.

3. Rouse-Segmental Motion as Probed by Depolarized Photon-Correlation Spectroscopy

The usual mode of photon-correlation spectroscopy–self-beating–is based on the condition that the scattered light field obeys Gaussian statistics.[118,119] This makes it particularly suitable and popular for probing dynamics in systems "populated" by Brownian particles as exemplified by the numerous studies of polymer chain dynamics in solutions.[27,120] Depolarized dynamic light scattering being much affected by the fast fluctuations of polarizability anisotropy, it is expected that depolarized photon-correlation spectroscopy mainly probes the reorientation motion of a correlated region.[121] Since the Rouse segment is the most basic Brownian particle in the Rouse model, which describes very well the polymer viscoelastic behaviour over at least the intermediate- and long-time regions of an entanglement-free concentrated system,[4,14,15] the depolarized photon-correlation function may provide the information about the motion of a single Rouse segment. Such an expectation is borne out by recent studies[9,10,21-23] as summarised below:

Depolarized photon-correlation spectroscopy was first used to study the chain dynamics in a well-entangled polystyrene melt by Patterson *et al.*[13] It was later pointed out by Lin[9,10] that the average correlation time $\langle \tau_c \rangle$ obtained by Patterson follows the same temperature dependence as that of viscosity of nearly monodisperse polystyrene samples obtained by Plazek and O'Rourke[122] from 130 to 110°C (see Figure 5; the correction for the changes in density and temperature as made in the figure causes only a negligible difference). The $\langle \tau_c \rangle$ value changing by a factor as large as 356 over this temperature range, the agreement is significant, suggesting strongly that the observed time constant is basically τ_v–i.e. of the same order of magnitude–as given by eq 7, which shares the same frictional factor K as that of viscosity (eq 6).

K of polystyrene at 127.5°C is given by the average value listed in Table 1 of ref. 11 to be $5.2 \times 10^{-9} \pm 10\%$. The structural factors of the relaxation times of the Rouse–Mooney normal modes $\{\tau_A^p\}$ are independent of molecular weight. At the same time, if the molecular weight is sufficiently high, K'/K is at the plateau value 3.3 based on eq 8 of ref. 11. The polystyrene sample studied by Patterson *et al*. was prepared by thermal polymerization at 90°C. Under such a condition, its number-average molecular weight is expected to be around 400,000; [123] in other words, it is in the highly entangled region where the plateau value of K'/K is applicable, even though its molecular-weight distribution is not nearly monodisperse. Thus, we can use the above K value at 127.5°C and the ratio K'/K =3.3 to obtain K'. As explained in ref. 11, the mass of a Rouse segment of polystyrene, m, being about 850,[6-12, 21-23,124,125] leads to N_e=16. Using the value of K' obtained as described above and N_e=16 or equivalently m=850 we can calculate $\tau_v \approx \tau_A$[15] from eq 7 or eq 5 (with K substituted by K'; and N_r replaced by N_e=16) to be 5.1×10^{-3} sec, which, clearly as expected, is of the same order of magnitude as the $\langle \tau_c \rangle$ value at 127.5°C, 3.5×10^{-3}, obtained from Patterson's results by interpolation.

In the case of polystyrene, it has been shown that the effective optical anisotropy per monomer unit from polystyrene in melt and in solution (cyclohexane as the solvent, whose

depolarized light scattering is negligible) is the same[126,127] indicating that the static correlation between segments belonging to *different chains* is nil. And the dynamic pair correlation is in general much smaller than the static pair correlation.[29,128] On the basis of neglecting both the static and dynamic pair correlation among segments belonging to different chains, and assuming that the size of the polymer coil is much smaller than the scattering wavelength and that the collective reorientation time is much shorter than the time needed for the centre-of-mass of the polymer chain to travel the distance of a scattering wavelength, the time-correlation function for depolarized Rayleigh light scattering can be expressed as.[9,10,21-23]

$$C(t) = \left[S\ f_s(t) + R\right]\left\langle P_2\left[\mathbf{u}(t)\cdot\mathbf{u}(0)\right]\right\rangle \qquad (8)$$

where P_2 is the second-order Legendre polynomial; $\mathbf{u}(t)$ is the unit vector representing the direction of the symmetry axis of a correlated region–the whole region is regarded as a Kuhn segment or equivalently a Rouse segment [129]–along the polymer chain at time t; $f_s(t)$ is a normalized time-correlation function that reflects the motions associated with the local chemical bonds, which are grossly referred to as the sub-Rouse-segmental motion; the relaxation strength S depends on the details of bond angles and steric interactions among chemical bonds; and R is a constant that is related to how anisotropic the correlated region is.

The depolarized photon-correlation functions of two entanglement-free concentrated solutions (~60wt%) of polystyrene with M_w=9100; M_w/M_n=1.02 and M_w=18100; M_w/M_n=1.01 in cyclohexane at the θ condition, i.e. at 35°C–denoted by samples S1 (59.832wt%; 0.552 g/cm^3) and S2 (60.287wt%; 0.556 g/cm^3), respectively–have been measured and analysed.[21-23] Along with the depolarized photon-correlation measurements, two solution samples with accurately determined concentrations in the close neighbourhood of the concentration of each of the two samples, S1 and S2, are prepared for viscosity measurements by the falling-ball method, which,

with both the ball and solution sealed in a glass tube, is particularly good for studying solution systems as solvent evaporation can be prevented. Then, by interpolation or extrapolation, the viscosity values at the concentrations of samples S1 and S2 can be individually determined; subsequently, their τ_v values can be calculated (eqs 6 and 7) for comparison with their depolarized photon-correlation results. Furthermore, the obtained information of the concentration dependence of viscosity allows the viscosity results to be compared under the same concentration and can be used to correct for the small concentration difference between samples S1 and S2 when their depolarized photon-correlation results are compared. The discussions below are all based on the results after the corrections have been made; the details of the corrections can be found in ref. 21.

The obtained molecular-weight dependence of viscosity at the same concentration (60 wt%) indicates that the Rouse theory is applicable; in other words, the concentrations of the studied polystyrene solutions are high enough to screen out the hydrodynamic interactions.[2] This conclusion is further confirmed by analyses in terms of the Rouse theory in other aspects of experiments as will be described below. Through the multi-exponential singular-value decomposition (MSVD) analysis,[27] a bimodal relaxation-time distribution can clearly be obtained from the depolarized photon-correlation functions of both S1 and S2, as corresponding to the two modes of motion in eq 8. Because of the limitation of the time window of photon-correlation spectroscopy, only the tail region of the fast mode $f_s(t)$ can be observed. Thus, as far as the fast mode is concerned, one can only show its existence from the MSVD analysis. However, much information about the slow mode $\langle P_2[\mathbf{u}(t)\cdot\mathbf{u}(0)]\rangle$ has been obtained from the analysis of the experimental results.[21-23] It has been shown that the slow mode, with a rather narrow relaxation-time distribution–extending over slightly less than two decades, is *independent of scattering angle and molecular weight* in accordance with eq 8. In the polystyrene melt case, the depolarized photon-correlation function is well described by the stretched exponential form with the stretching exponent β near 0.4. This corresponds to a

unimodal broad relaxation-time distribution, covering more than five decades.[130] The fact that the two modes of motion as contained in eq 8 cannot be separated in melt as in the concentrated-solution case is explained as due to the stronger interactions among segments causing the two modes to overlap extensively.

Assuming $\mathbf{u}(t)=\mathbf{b}(t)/|\mathbf{b}(t)|$, the time-correlation function $\langle P_2[\mathbf{u}(t)\cdot\mathbf{u}(0)]\rangle$ can be calculated by the Monte-Carlo simulation based on the Langevin equation of the Rouse model.[4,22] Also, from the simulation, the ratio between τ_v (corresponding to eq 7) and the average correlation time $\langle\tau\rangle_r$ obtained from integrating the simulated $\langle P_2[\mathbf{u}(t)\cdot\mathbf{u}(0)]\rangle$ curve can be calculated for comparison with the experimental results $\langle\tau\rangle_2/\tau_v$ ($\langle\tau\rangle_2$ denotes the average correlation time of the slow mode obtained from resolving the measured photon-correlation function, while τ_v is calculated from the viscosity data through eqs 6 and 7). In comparing the analyses of the depolarized photon-correlation function, viscosity and Monte-Carlo simulation results, we have found that m=1130 gives a good overall agreement: Corresponding to m=1130, N_r=8 and 16 for samples S1 and S2, respectively. From the results of the depolarized photon-correlation function and viscosity, we obtained $\langle\tau\rangle_2/\tau_v$=2.4 and 2.6 for samples S1 and S2, respectively; from the simulation, we obtained $\langle\tau\rangle_r/\tau_v$=2.2 and 2.5 for N_r=8 and 16, respectively. Furthermore, as shown in Figure 1, the line shapes of the time-correlation functions of the slow mode of both samples S1 and S2 (denoted by $\langle C_2(t)\rangle$) are in close agreement with the simulation results of $\langle P_2[\mathbf{u}(t)\cdot\mathbf{u}(0)]\rangle$ for N_r=8 and 16. Thus, in spite of the crudeness of the Rouse segment, the effect of chain connectivity as contained in the Rouse model can quite fully account for the detailed aspect of the dynamics as showing up in the depolarized photon-correlation function and its relation with viscosity, supporting the physical picture that the dynamic process probed by depolarized photon-correlation spectroscopy is the reorientation motion of a Rouse segment. The mass of a Rouse segment obtained for the studied concentrated polystyrene solutions, m=1130, is about 25% larger than that in the melt. This small difference should be due to the presence of solvent; indeed, the small solvent-enhancement effect is about that expected from the

concentration-dependence of the Rouse segment size obtained by Inoue *et al.*[12] from analyzing the dynamic mechanical and birefringence results–the expected *m* value at the studied concentration is about 1100, versus 850 in the melt (see Figure 10 of ref. 12). The agreement between the two independent studies based on very different premises[131] reconfirms that the Rouse segment size can be defined and that the motion associated with a single Rouse segment can indeed be studied; in other words, the study of the Rouse-segmental motion as presented above is well supported.

In summing up the above studies of polystyrene melt and concentrated solutions, we can notice differences and common points: The differences between the melt case and the concentrated-solution case are mainly two: (1) The relaxation-time distribution is much broader in the former than in the latter, and (2) the $\langle \tau_c \rangle / \tau_v$ ratio is smaller in the former than in the latter (denoted by $\langle \tau \rangle_2 / \tau_v$ in the latter case). These two differences can be accounted for by the stronger interactions among segments in the melt–in the concentrated-solution case, the interactions among segments can be much reduced by the "lubrication" of the solvent molecules. Due to the stronger interactions in the melt case, the fast and slow modes as contained in eq 8 overlap extensively; the photon-correlation function cannot be resolved into the two modes. While the effect leads to a broad unimodal relaxation-time distribution,[13,38] the fast component in the distribution also causes the observed average relaxation time $\langle \tau_c \rangle$ to be smaller than when only the slow component contributes to it as in the concentrated-solution case. The main shared common point is the applicability of the Rouse model–either as $\mu_R(t/\tau_R)$ or as $\mu_A(t/\tau_A)$, which is a part of ERT–in relating the viscoelasticity results to the dynamics observed by depolarized photon-correlation spectroscopy. As the melt system and the concentrated-solution system at the θ point are very similar dynamically and thermodynamically–both free of the hydrodynamic interactions and excluded-volume effect,[2] the precise analysis achieved in the concentrated-solution case lends additional support to the analysis of the melt results, in which some of the details are prevented by the much broader relaxation-time distribution in $C(t)$ from being

revealed.

In summary, the recent studies as briefly described above confirm the initial expectation that the motion of a single Rouse segment can be studied by depolarized photon-correlation spectroscopy. This conclusion has a bearing on the comparison of the α relaxation with the highest Rouse–Mooney normal mode, both extracted from the creep compliance $J(t)$ as reported in ref. 11.

4. The α Relaxation in Creep Compliance

With $G(t)$ known—for instance as given by eqs 1, 4 and 5 of ref. 11—$J(t)$ can be calculated numerically by the method of Hopkins and Hamming.[132,133] It has been shown in detail in ref. 11 that the rubber(like)-fluid region of Plazek's $J(t)$ results of two nearly monodisperse polystyrene samples [134,135] can be well described by ERT and that the dynamic information of the glassy-relaxation process as contained in the small-compliance/short-time region of $J(t)$ can be meaningfully extracted by using the successful description of the rubber(like)-fluid region in terms of ERT as the reference frame. The glassy-relaxation process is found to be well described by the stretched exponential form

$$A_G \mu_G (t/\tau_G) = A_G \exp\left[-\left(\frac{t}{\tau_G}\right)^{\beta}\right] \qquad (9)$$

as incorporated into eq 4 of ref 11. In the whole relaxation-time distribution, the glassy-relaxation region is situated in a certain position relative to the rubber(like)-fluid region, where all the relaxation times are proportional to the frictional factor K. The relative position has been expressed by

$$\langle \tau \rangle_G = sK \qquad (10)$$

where s is a proportional constant and has the unit of Dalton square. The parameter s represents the glassy-relaxation time with K fixed at 1 or any constant; it is regarded as a normalized glassy-relaxation time. In the vicinity of T_g, the parameter s increases with decreasing temperature, reflecting the thermorheological complexity between the glassy-relaxation process, $A_G\mu_G(t)$, and the ERT processes: $\mu_A(t)$, $\mu_X(t)$, $\mu_B(t)$, and $\mu_C(t)$, in the rubber-fluid region and indicating the existence of a structural length scale as discussed in detail in ref. 11.

Sample B whose $J(t)$ results was analyzed in ref. 11 is contaminated by residual plasticizers; the K value extracted from it cannot be used for comparing with studies on normal (uncontaminated) samples. Thus, in this report, we only discuss the results of sample A. It has been found for sample A that A_G (=5482) and the stretching parameter β (=0.41) are very much independent of temperature, while s increases with decreasing temperature significantly–by about an order of magnitude over the covered temperature range. The obtained K and s values at different temperatures for sample A are listed in Table 1. Using the obtained K and s values in the τ_A^p equation (i.e. eq 5 with K replaced by K'=1.61K as calculated from eq 8 of ref. 11 for M=4.69x10^4; M replaced by M_e; and N_r replaced by N_e=16) and eq 10, the $\tau_v \approx \tau_A^{15}$ and $\langle \tau \rangle_G$ values at different temperatures can be, respectively, calculated, as also shown in Table 1.

One may calculate the $J(t)$ curves at different temperatures *in real time* with the K and s values shown in Table 1. Instead of doing this way, the comparisons of the $J(t)$ curves of sample A measured at different temperatures to those calculated with K fixed at 5x10^{-9} and the s values listed in Table 1 are shown in Figure 1 of ref. 11. This illustrates using the description of the rubber(like)-fluid region of $J(t)$ in terms of ERT as the reference frame to show the effect of temperature on the glassy-relaxation process; such a comparison serves the purpose of reflecting and characterizing in perspective the thermorheological complexity occurring in $J(t)$ as the temperature is near T_g. As also shown in ref. 11, unlike the extensive overlapping of the

different processes in $J(t)$, the individual processes can be clearly shown in the $G(t)$ form. Based on the $G(t)$ results, a structural relaxation time τ_S was defined as the time when G/R has declined to 3 as described in detail in ref. 11. The thus defined structural relaxation time becomes greater than τ_v just before the temperature reaches T_g, indicating vitrification at the Rouse-segmental level.

As will be shown below, the structural relaxation time defined by G/R =3 can be considered as basically equivalent to the so-called α-relaxation time. In the literature, the α-relaxation time has been "defined" in different ways,[5,136] such as the reciprocal of the frequency at the peak of tan δ and the reciprocal of the frequency at which the storage modulus $G'(\omega)$ is at 10^8 dyn/cm^2. The relaxation time defined in any of these ways can in principle be determined clearly by experiment. However, it does not really characterizes a relaxation process in a simple and clear manner; with a temperature change, it is affected not only by the intrinsic temperature dependence of the relaxation process that matters but also by the change in the line shape of the viscoelastic spectrum–namely, the thermorheological complexity. The structural relaxation time defined as the time when G/R=3 has a similar defect.

To further illustrate the physical effect on the bulk mechanical property by the glassy relaxation, another analysis will be made below. This analysis confirms the basic physical uniqueness of τ_S as defined by the time when G/R=3. Based on these findings, an optimum definition for τ_S is chosen, which has an unambiguous meaning in its temperature dependence and at the same time properly reflects the effect on the bulk property by the glassy relaxation. And it will be shown below that the thus defined τ_S is very close to the α-relaxation time defined by one of the traditional ways.

We consider that the time when the absolute value of the slope $d(\log G(t))/d(\log t)$, denoted by H, reaches its first maximum reflects a unique physical meaning associated with the glassy-relaxation process as explained in the following: As shown previously and mentioned above, the $\mu_G(t)$ process can be well described by the stretched exponential form with β=0.41,

which is very much independent of temperature. In the high-modulus/short-time region where the glassy-relaxation process dominates,

$$H = \left| \frac{d(\log G(t))}{d(\log t)} \right| = \beta \left(\frac{t}{\tau} \right)^{\beta} \qquad (11)$$

As shown in Figure 2, initially following eq 11, log H increases with log t with a slope of β=0.41, indicating a gradually steeper decline of log $G(t)$ with log t. At the time, denoted by t_m, when H reaches its first maximum, while the *rate* of the glassy-relaxation process has the greatest influence, its modulus magnitude is losing its dominance as deviation from eq 11 begins taking place. As it turns out, the location of the H maximum occurs in the neighbourhood of the structural relaxation time defined as the time when G/R=3. The obtained t_m values at different temperatures are listed in Table 1, which occur in the range of 15~25 $\langle \tau \rangle_G$, depending on the temperature. The obtained $\langle \tau \rangle_G$ values occur in the too short-time region to clearly reflect the dynamic effect of the glassy-relaxation process on the bulk mechanical property; however, they carry the intrinsic temperature dependence of the glassy-relaxation process. To have the benefits of both t_m and $\langle \tau \rangle_G$, we redefine the structural relaxation time arbitrarily as τ_S=18$\langle \tau \rangle_G$, whose values at different temperatures are also listed in Table 1. Allowing a 20% deviation from this somewhat arbitrarily chosen τ_S—for instance one may as well choose τ_S=22$\langle \tau \rangle_G$—the main point that will be explained in terms of the defined τ_S remains the same.

For comparing the above-defined τ_S with the α-relaxation time defined in the literature, the storage-, loss-modulus and tan δ spectra of sample A are shown in Figures 3 and 4, all the spectra being "normalized" with respect to K=5x10^{-9} (see the Appendix for the calculations of the spectra). As, being basically a mirror image, the $G'(\omega)$ spectrum has a close match to $G(t)$ if ω=0.7/t is used in the conversion between time and frequency, we define ω_S=0.7/τ_S.[137] The thus defined ω_S values at 114.5, 104.5 and 97°C are compared in Figure 4 with what have been

used traditionally: at the peak of tan δ and at $G'(\omega)=10^8$ dyn/cm^2. It can be seen that the ω_S values at the three shown temperatures occur in the close neighbourhood of the frequencies where the respective storage-modulus has the value 10^8 dyn/cm^2; however, they deviate considerably from the respective frequencies at the tan δ maximum. In a case where a careful analysis as done in this study is not feasible, using $G'(\omega)=10^8$ dyn/cm^2 as the criterion for deciding the α-relaxation time may be a good choice except bearing that the thus determined relaxation time does not follow exactly the temperature dependence of $\langle\tau\rangle_G$ as the above defined τ_S does.

In Figure 4, the frequency corresponding to the highest Rouse–Mooney normal mode, $\omega_v=0.7/\tau_v$, is also indicated. One can see that at a temperature between 104.5 and 97°C, ω_S becomes smaller than ω_v, signalling the initiation of vitrification at the Rouse-segmental level, a prelude to the glass transition. This was pointed out in terms of the previously defined structural-relaxation time,[11] which reflected the similar effect of the glassy-relaxation process. In fact, as values of the previously defined τ_S at different temperatures are very close to the values based on the present definition (see Table 2 of ref. 11), the discussion of the physical role of the structural relaxation in terms of τ_S defined by $G/R=3$ remains essentially the same as in terms of the above defined τ_S, which has the additional advantage that, as shown below, its temperature dependence can be unambiguously compared with those of other dynamic quantities.

5. Comparison of the Temperature Dependences of Various Dynamic Quantities

For showing the chain dynamics in the polystyrene melt in perspective, the above analyses and discussions of the depolarized photon-correlation results and the creep compliance $J(t)$ can be put together by comparing the temperature dependences of the obtained dynamic quantities. The comparison, while confirming the validity of the physical picture in terms of which we have extensively analysed the experimental results, summarizes the different physical roles as represented by these dynamic quantities.

Shown in Figure 5 are the $\langle \tau_c \rangle$ values obtained by Patterson;[13] the values of τ_v and τ_S as listed in Table 1; the temperature dependence of the viscosity corrected for changes in density and temperature, $\eta/\rho T$;[30,42] and the temperature dependence of the recoverable compliance $J_r(t)$ obtained by Plazek.[30,42] It is clear from the comparison that these dynamic quantities follow two distinctly different modes of temperature dependence: One, being steeper, is followed by τ_S and $J_r(t)$; the other one is followed by τ_v, $\langle \tau_c \rangle$, and $\eta/\rho T$. In Figure 5, the unit scale on the vertical axis is for τ_v and τ_S; the shown $\langle \tau_c \rangle$ points represent Patterson's values multiplied by 0.77;[138] and the $\eta/\rho T$ values and the shift factors in $J_r(t)$, as shown, have been individually multiplied by a proper factor so that they are superposed closely on the data points of τ_v and τ_S, respectively. In the figure one can note that the temperature dependence of $\langle \tau_c \rangle$ above ~110°C is parallel with and below ~110°C becomes less steep than that of τ_v and $\eta/\rho T$. The reason for the divergence below ~110°C will be explained below. In the steeper mode, the temperature dependence of τ_S and that of $J_r(t)$ are closely parallel with each other, representing the consistency between the two means of obtaining the temperature dependence of the creep compliance $J(t)$ in the small-compliance/short-time region: One is obtained from the analysis of the $J(t)$ results in terms of the combination of eqs 1, 4 and 5 of ref. 11, while the other is obtained through empirical data reduction by Plazek.[30,42]

The temperature dependence of η is calculated using the equation obtained by Plazek and O'Rourke[30,42] from the least square fitting to the data of sample A measured in the region $\geq$104.5°C. This temperature dependence is in close agreement with those of other nearly monodisperse samples with a higher molecular weight to the lowest temperature–always higher than 104.5°C–which is covered by the viscosity measurements of each individual sample.[30] As τ_v, being calculated from K, reflects the temperature dependence of K and the zero-shear viscosity is dominated by the dynamic processes whose temperature dependence is determined by K–the contribution from $A_G\mu_G(t)$ being in general negligibly small, the temperature

dependence of τ_v and that of $\eta/\rho T$ agree closely above 104.5°C. With the guidance of the calculated $J(t)$ curves, the frictional factor K, which is used to calculate the τ_v value, can be determined at a temperature as low as the calorimetric T_g (see Figure 1 of ref. 11). As opposed to this, the viscosity of sample A could be determined only down to 104.5°C.[30,42] However, below 104.5°C, the extended $\eta/\rho T$ curve based on the same viscosity equation and the τ_v data points still have a good agreement. The agreement between the temperature dependences of τ_v and $\eta/\rho T$ as described above supports that the K values listed in Table 1 have been correctly determined. To examine the comparison more closely, one may notice that when the temperature is close to T_g, the $A_G\mu_G(t)$ contribution to the zero-shear viscosity becomes slightly noticeable in the flow region of the $J(t)$ curve (see Figure 1 of ref. 11)–because the s value becomes large and, due to the molecular weight being not large, the terminal region of sample A is not far away in time. This effect may account for the slight tilt-up of the $\eta/\rho T$ curve in comparison to the τ_v points at temperatures close to 104.5°C as vaguely suggested in Figure 5. As the effect is very small, the temperature dependence of τ_v and $\eta/\rho T$ is treated as the same in most discussions in this report.

The steeper temperature dependence of τ_S (or $J_r(t)$) in comparison with that of τ_v (or $\eta/\rho T$) reflects the thermorheological complexity in $J(t)$. At slightly above 100°C, τ_S crosses over τ_v, signalling vitrification at the Rouse-segmental level. The crossing over is illustrated here in the real time scale as opposed to that shown in Figure 4 in a normalized time scale.

As pointed out above, the temperature dependence of $\langle \tau_c \rangle$ becomes less steep than that of τ_v below 110°C, indicating surely that the dynamics observed by depolarized photon-correlation spectroscopy cannot be associated with the α- or glassy-relaxation process, whose temperature dependence is steeper than that of τ_v. Furthermore, the glassy-relaxation process should very much involve strong interactions among segments belonging to different chains; in contrast, the effective optical anisotropy per monomer unit of polystyrene in bulk and in solution is the same

indicating that the dynamics probed by depolarized photon-correlation spectroscopy does not involve correlation between segments of different chains. Theoretically, one should not expect such an association either, as the photon-correlation measurement is based on the condition that the optical field obeys Gaussian statistics, requiring that the studied system be ergodic; as opposed to this, the emerging greater role of the glassy-relaxation process causes the loss of effective ergodicity as the temperature approaches T_g. While the parallel temperature dependence between $\langle \tau_c \rangle$ and τ_v (or $\eta/\rho T$) above 110°C supports associating the dynamic process observed by depolarized photon-correlation spectroscopy with the motion of a Rouse segment, as discussed in Section 3; below ~110°C, the gradual loss of ergodicity can have an effect on the dynamics as actually probed by depolarized photon-correlation spectroscopy. Especially, since the longest delay-time used in the photon-correlation measurement by Patterson *el al.*[13] is 1 sec., the loss of effective ergodicty is a factor that cannot be ignored as τ_S exceeds 1sec. at around 107°C and the actually measured $\langle \tau_c \rangle$ value exceeds 1sec. at just slightly below 110°C. As shown by Pusey and van Megan,[139] if the intensity correlation function measured on a non-ergodic medium is analysed by the method normally used for an ergodic medium, the *apparent* rate so obtained can be greater than the real rate by a large factor. The factor of course depends on how severe the loss of effective ergodicity is. Applying Pusey and van Megan's analysis here, the apparent $\langle \tau_c \rangle$ values obtained by Patterson *et al*. are expected to be smaller than the real values below 110°C, where some loss of effective ergodicity begins to occur as explained above. This effect explains the weaker temperature dependence of $\langle \tau_c \rangle$ in comparison with that of $\eta/\rho T$ or τ_v below ~110°C as shown in Figure 5.

6. Summary

Because of the large number of atoms and degrees of freedom in a chain molecule, a polymer is rich in its dynamics, with its relaxation-time distribution covering many decades. Different probing techniques are sensitive to different aspects of chain dynamics. To understand

the chain dynamics in perspective, it is advisable to use different probing techniques to investigate the same (kind of) system; at the same time, it is desirable to relate the data obtained by the different techniques to one another through theoretical analyses and/or simulations. In this report together with the previous one, we show how the results of polystyrene obtained by the viscoelasticity and depolarized photon-correlation measurements are combined, giving a comprehensive picture of the dynamic processes in the short-time region. The basic reason for the two techniques being particularly complementary to each other is that both probe the Brownian motion. From a preliminary analysis of experimental results it was shown that the dynamics in polystyrene melt probed by depolarized photon-correlation spectroscopy should reflect the motion associated with a single Rouse segment. In the case of the concentrated polystyrene solution, the analysis benefiting from the Monte Carlo simulation has a high resolution confirming in a precise manner the interpretation of the depolarized photon-correlation results. By this it demonstrates that the size of a Rouse segment can be defined experimentally–in agreement with Inoue *et al.*[6-8,12]–and that its motion can be studied. That the temperature dependence of $\langle \tau_c \rangle$ is parallel with that of τ_v rather than that of τ_S is a logical consequence. As much discussed in the previous paper,[11] using the description of the Brownian dynamic processes in $J(t)$ in terms of ERT as the reference frame in the analysis over the whole range, the glassy-relaxation process–namely, the α relaxation–is characterized, showing that the thermorheological complexity in $J(t)$ as first observed by Plazek is closely related to the loss of ergodicity in approaching T_g. The temperature dependence of $\langle \tau_c \rangle$ becoming less steep than that of τ_v below 110°C can be explained as due to the increasing loss of effective ergodicty when the temperature is lowered towards T_g.

In this study we have examined the Rouse-segmental motion in polystyrene as probed by depolarized photon-correlation spectroscopy in the light of the information obtained from the analysis of the $J(t)$ results as reported in the previous paper. It shows that the α relaxation and the motion associated with a single Rouse segment are closely buried in the transition

region–actually crossing each other just before reaching the calorimetric T_g. As a result, it is easy to mistake one for the other. This study has also proposed a way to define the α-relaxation time in polystyrene, with a clear physical meaning. Whether the same can be equally applied to other polymers remains to be seen.

Acknowledgement

This work is supported by the National Science Council (NSC 92-2113-M-009-027).

Appendix: Calculations of the Spectra of $G'(\omega)$, $G''(\omega)$ and tan δ (Note: in this appendix, all the equations referred to are those in **ref. 11**)

The spectra of storage and loss modulus and loss tangent of sample A as shown in Figures 3 and 4 are calculated by obtaining first its relaxation-time distributions at different temperatures as contained in the $G(t)$ curves shown in Figure 5 of ref. 11. The $G(t)$ curves have been calculated from the combination of eqs 1, 4, 5 and 7 using the parameters A_G, β and s extracted from the analysis of the measured $J(t)$ curves. In all the calculations described below, the effect of the molecular-weight distribution of the sample has been taken into account in the same way as explained in the analyses of $J(t)$[11] and calculations of $G(t)$.[4,16-18] To obtain the relaxation-time distribution of sample A, we can first consider two portions in eqs 1 and 4 separately: One is the part corresponding to ERT, namely, the portion without the $A_G\mu_G(t)$ term. The other is the $A_G\mu_G(t)$ term as contained in eq 4. In the former, all the theoretical forms of the relaxation processes and their relaxation times are known. Thus, for this portion a computer program can be constructed to accumulate the relaxation strengths of all the coupled or composite processes (arising from the product of two or three exponentially-decaying functions) with relaxation times that fall in a small time-interval, $\Delta\log t$, equally spaced in the log t scale, giving the relaxation-time distribution with a resolution as high as one practically desires. On the other hand, the relaxation-time distribution of the $A_G\mu_G(t)$ term with $\mu_G(t)$ given by eq.5 can

be calculated numerically.[38] For the present calculations, the resolution of 100 subdivisions per decade has been used throughout, which is more than ample. The total relaxation-time distribution can be formed from the distributions obtained for the two separate portions in accordance with the theoretical form as given by eqs 1 and 4. The obtained total relaxation-time distribution is first checked by calculating numerically the $G(t)$ curves for comparison with those calculated from eqs 1, 4 and 5 directly, i.e. those shown in Figure 5 of ref. 11. Absolutely no discrepancy can be noticed between the two sets of $G(t)$ curves. With the relaxation-time distributions confirmed this way, the spectra of storage and loss modulus, and thus of loss tangent can be calculated numerically in a straightforward manner. This approach of calculating $G'(\omega)$, $G''(\omega)$ and $\tan\delta$ from $G(t)$–free of the approximation that is often involved in the conversion between the time and frequency domains[5]–is possible only because the theoretical form of $G(t)$ is known. As the measurement conditions–such as the use of the frictionless magnetic bearing and the control of temperature–in the creep experiment by Plazek are far more stringent than normally taken, the shown $G'(\omega)$, $G''(\omega)$ and $\tan\delta$ spectra derived faithfully from the quantitative description of Plazek's $J(t)$ results should be much more reliable than ever obtained directly from a strain-controlled measurement.

Figure Captions:

Figure 1.

Comparison of the $\langle P_2\,[\mathbf{u}(0)\cdot\mathbf{u}(t)]\rangle^2$ dynamic processes obtained from the depolarized photon-correlation functions of the S1 (◦)and S2 (•) samples and the simulation results of the Rouse chain with N_r=8 (the left solid line) and with N_r=16 (the right solid line).

Figure 2

H indicating the declining rate of log $G(t)$ vs. log t, as defined in the text, is shown as a function of time for sample A at 114.5, 109.6, 104.5, 100.6, and 97^{o}C corresponding to lines from left to right, respectively; all calculated with K fixed at $5\text{x}10^{-9}$ and the respective s values listed in Table 1.

Figure 3

Comparison of the storage- and loss-modulus spectra, $G'(\omega)$ and $G''(\omega)$, of sample A at 114.5 (——), 104.5 (– · –), and 97^{o}C (–··–) all calculated with K fixed at $5\text{x}10^{-9}$ and the respective s values listed in Table 1.

Figure 4

Comparison of the storage-modulus (——) and loss-tangent (– – –) spectra of sample corresponding to those shown in Fig. 3: a for 114.5^{o}C, b for 104.5^{o}C and c for 97 ^{o}C. Also shown are the $\omega_S=0.7/\tau_S$ values (right ↓ for a; middle ↓ for b; left ↓ for c) calculated with K fixed at $5\text{x}10^{-9}$ and the respective s values listed in Table 1; and the $\omega_v=0.7/\tau_v$ value (↑) calculated with the same K. The upper dotted line is $G''(\omega)$ calculated without the $A_G\mu_G(t)$ term; the lower dotted line is calculated without both $A_G\mu_G(t)$ and $\mu_A(t)$.

Figure 5

Comparison of τ_v (●), $0.77\langle\tau_c\rangle$ (■) and τ_S (○) as a function of temperature with the temperature dependence of $\eta/\rho T$ (——; the extended line below 104.5°C is indicated by · · ·) and $J_r(t)$ (– · – · –); see the text.

TABLE 1: The Values of K, s, τ_v, $\langle\tau\rangle_G$, t_m and τ_S of Sample A (M_w=4.69x10^4) at Different Temperatures[+]

t °C	K	s	τ_v	$\langle\tau\rangle_G$	t_m	τ_S
127.5	4.8×10^{-9}		2.28×10^{-3}			
125	9.08×10^{-9}		4.3×10^{-3}			
114.5	1.96×10^{-7}	6283	9.3×10^{-2}	1.23×10^{-3}	1.78×10^{-2}	2.21×10^{-2}
109.6	1.2×10^{-6}	10053	.569	1.21×10^{-2}	.186	.218
104.5	1.2×10^{-5}	16337	5.69	.196	3.39	3.53
100.6	9.7×10^{-5}	28275	46	2.74	56.2	49.4
97	9.84×10^{-4}	56550	467	55.6	1349	1002

[+] All relaxation times are in unit of sec.

Figure 1

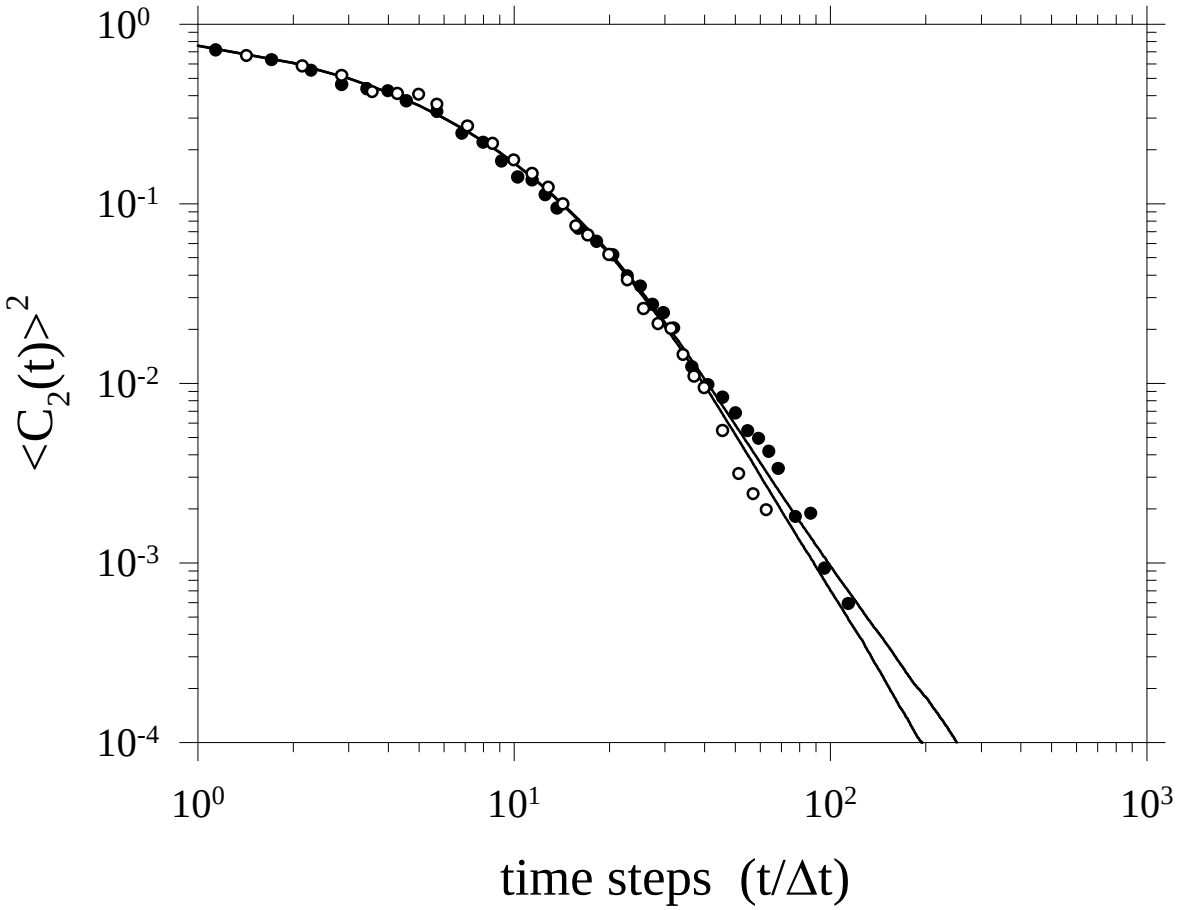

Figure 2

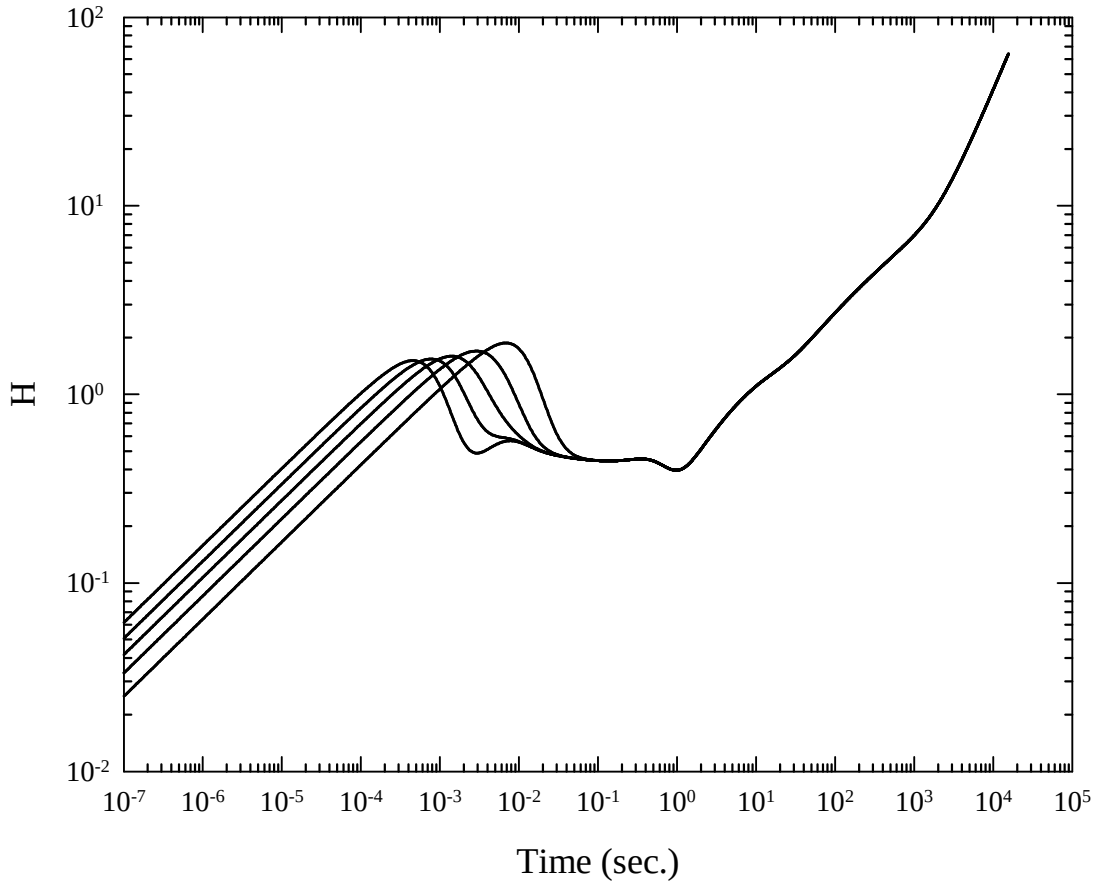
H
Time (sec.)
10^2
10^1
10^0
10^-1
10^-2
10^-7
10^-6
10^-5
10^-4
10^-3
10^-2
10^-1
10^0
10^1
10^2
10^3
10^4
10^5

Figure 3

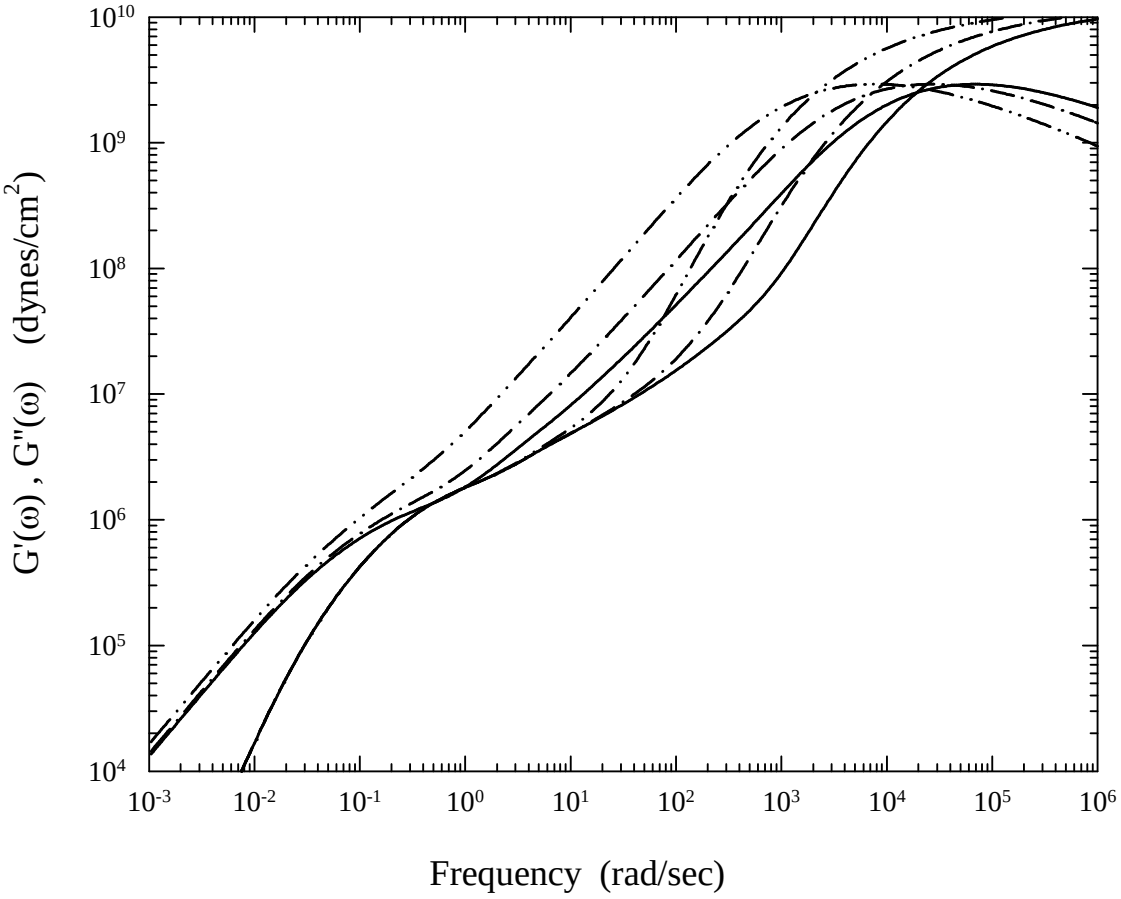
10^{10}
10^{9}
10^{8}
10^{7}
10^{6}
10^{5}
10^{4}
G'(ω) , G"(ω) (dynes/cm^2)
10^{-3}
10^{-2}
10^{-1}
10^{0}
10^{1}
10^{2}
10^{3}
10^{4}
10^{5}
10^{6}
Frequency (rad/sec)

Figure 4

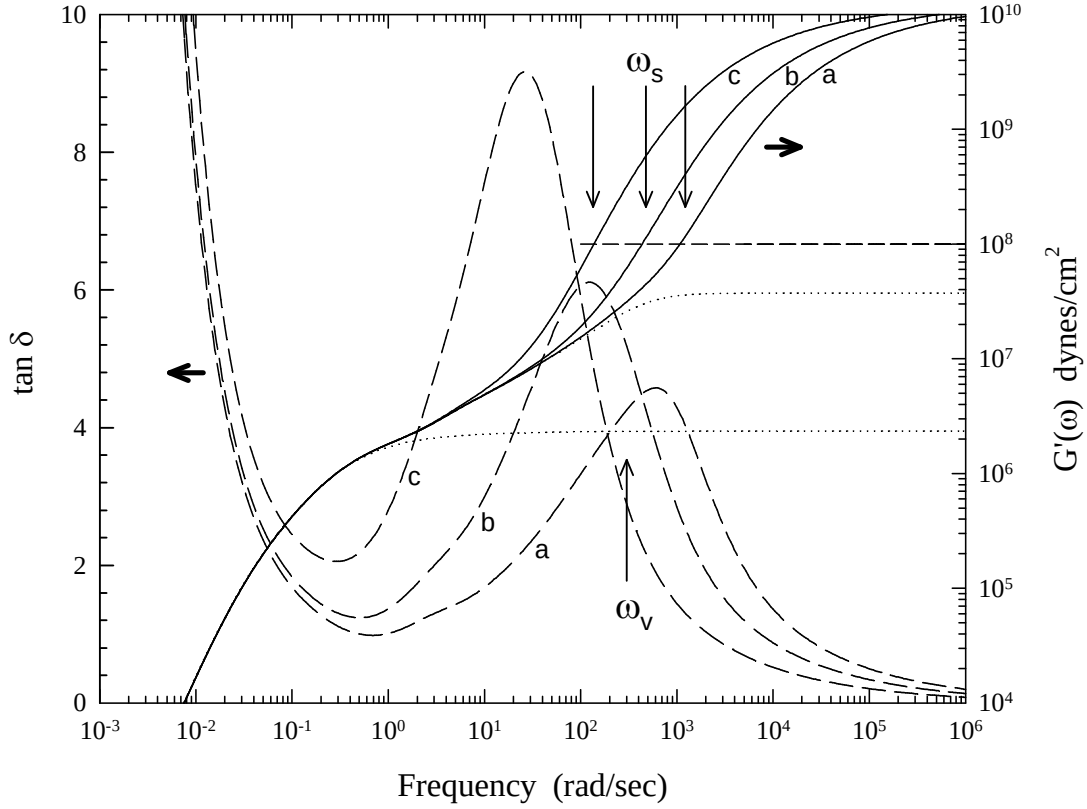
tan δ
G'(ω) dynes/cm²
Frequency (rad/sec)
ω_s
ω_v
a
b
c
10
8
6
4
2
0
10⁻³
10⁻²
10⁻¹
10⁰
10¹
10²
10³
10⁴
10⁵
10⁶
10¹⁰
10⁹
10⁸
10⁷
10⁶
10⁵
10⁴

Figure 5

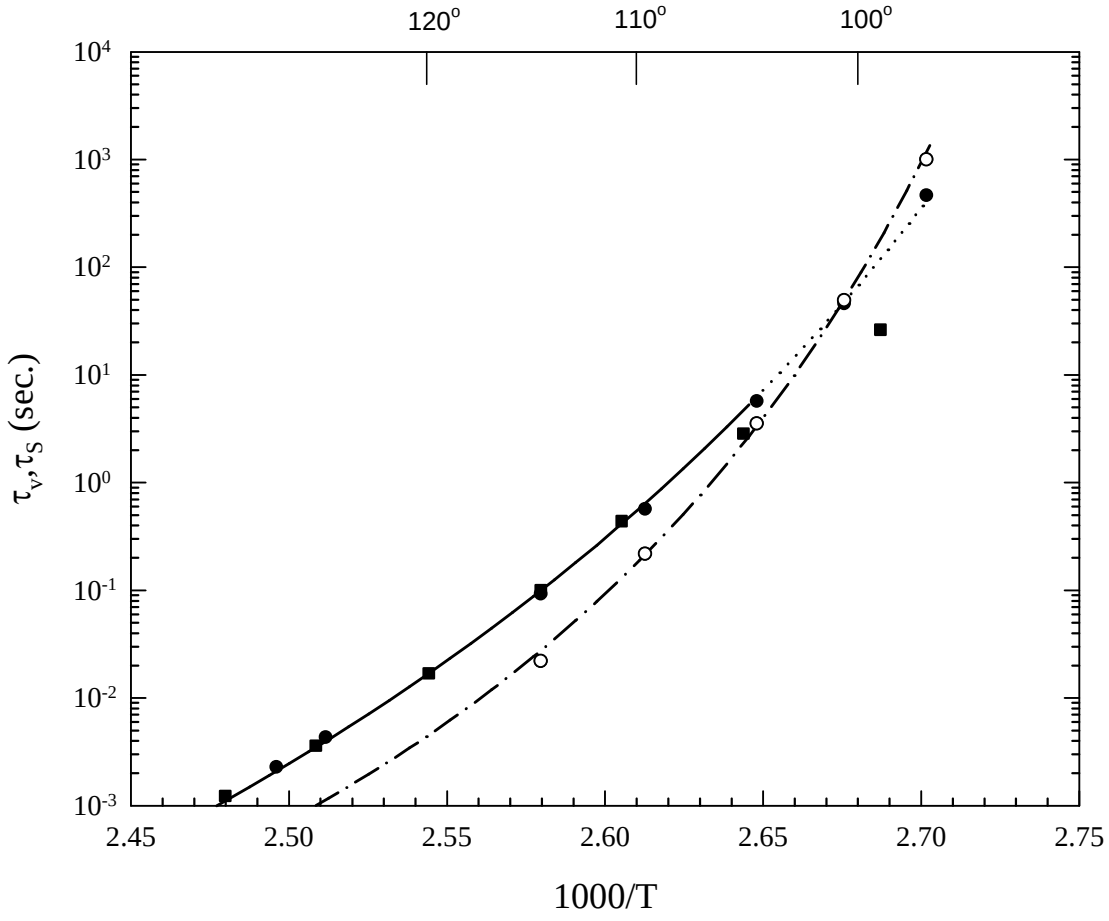
120°
110°
100°
10⁴
10³
10²
10¹
10⁰
10⁻¹
10⁻²
10⁻³
τv, τS (sec.)
2.45
2.50
2.55
2.60
2.65
2.70
2.75
1000/T

References and Notes of Report a

1 Ferry, J. D. *Viscoelastic Properties of Polymers*, 3rd ed.; Wiley: New York, 1980.

2 Lin, Y.-H. *Macromolecules* **1986**, *19*, 159.

3. Lin, Y.-H. *Macromolecules* **1986**, *19*, 168.

4. Lin, Y.-H. Lin *Macromolecules* **1987**, *20*, 885.

5. Lin, Y.-H. *Polymer Viscoelasticity: Basics, Molecular Theories, and Experiments*; World Scientific: Singapore, 2003.

6 Lin, Y.-H. *Macromolecules* **1991**, *24*, 5346.

7. Doi, M.; Edwards, S. F., *J. Chem. Soc., Faraday Trans. 2* **1978**, *74*, 1789; **1978**, *74*, 1802.

8 Lin, Y.-H. *Macromolecules* **1984**, *17*, 2846.

9 Note: In this paper, the term "rubber(like)-fluid" is often used to indicate the time region where the description in terms of ERT is applicable. The time region where ERT is applicable is technically slightly different between the line-shape analysis of $G(t)$ and that of $J(t)$. The difference arises from the fact that the $J(t)$ time region which corresponds to the Rouse–Mooney rubber region in $G(t)$ (the $\mu_A(t)$ process region) is much affected or "contaminated" by the glassy-relaxation process $A_G\mu_G(t)$ as shown in Figure 4. Thus, while in $G(t)$ the line shape of the rubber-fluid region is uniquely analysed in terms of ERT; in $J(t)$ only the rubberlike-fluid region is independently analysed in terms of ERT. Thus in "rubber(like)-fluid," the term "rubber" is meant for $G(t)$, while "rubberlike" is meant for $J(t)$. Since the frictional factor K is determined by the dynamics in the rubberlike-fluid region, the frictional

factor K values obtained from $G(t)$ and $J(t)$ as shown in Table 1 are independent of each other. However, the glassy-relaxation process extracted from $J(t)$ as shown in this study is based on the information of the $\mu_A(t)$ process obtained from the $G(t)$ line-shape analysis. Thus, when the term "rubber(like)" is used for $J(t)$, it means that the information of the $\mu_A(t)$ process obtained from the $G(t)$ line-shape analysis (i.e. eq 8) has been used when the $J(t)$ line-shape analysis over the whole range is being made, whose results are shown in Figures 1 and 2.

10 Ballard, D. G. H.; Rayner, M. G.; Schelten, J. *Polymer* **1976**, *17*, 349.

11. Norisuye, T.; Fujita, H. *Polymer J.* **1982**, *14*, 143.

12 Inoue T.; Okamoto, H.; Osaki, K. *Macromolecules* **1991**, *24*, 5670.

13 Inoue, T.; Hayashihara,H.; Okamoto, H.; Osaki, K. *J. Polym. Sci. Polym. Phys. Ed.* **1992**, *30*, 409.

14 Inoue, T.; Osaki, K. *Macromolecules* **1996**, *29*, 1595; Inoue, T.; Uematsu, T.; Osaki, K. *Macromolecules* **2002**, *35*, 820.

15 Lin,Y.-H. *J. Polym. Res.* **1994**, *1*, 51.

16 Lin, Y.-H.; Lai, C. S. *Macromolecules* **1996**, *29*, 5200.

17 Lai, C. S.; Juang, J.-H.; Lin, Y.-H. *J. Chem. Phys.* **1999**, *110*, 9310.

18. Lin, Y.-H.; Luo, Z.-H. *J. Chem. Phys.* **2000**, *112*, 7219; Lin, Y.-H. *J. Chin. Chem. Soc.***2002**, *49*, 629.

19 Plazek, D. J. *J. Phys. Chem.* **1965**, *69*, 3480.

20. Plazek, D. J. *J. Polym. Sci. A-2* **1968**, *6*, 621.

21. Note: The polydispersity of the sample, even though nearly monodisperse, has an

effect on the detailed line shape of $J(t)$ in the rubberlike-fluid region. This effect, as can be easily accounted for by convolution with the Schulz distribution, virtually does not affect the obtained K value. See Section 3.4.

22. Hopkins, I. L.; Hamming, R. W. *J. Appl. Phys.* **1957**, *28*, 906; *J. Appl. Phys*. **1958**, *29*, 742.

23. Tschoegl, N. W. *The Phenomenological Theory of Linear Viscoelastic Behavior*; Springer-Verlag: Berlin, 1989.

24. Mooney, M. *J. Polym. Sci.* **1959**, *34*, 599.

25. Doi, M. *J. Polym. Sci., Polym. Phys. Ed*. **1980**, ***18***, 1005.

26. Note: the relaxation times in the Rouse–Mooney-rubber region, τ_A^p, are proportional to K' which is in turn proportional to K through eq 8.

27. Schulz, G. V. *Z. Physik. Chem., Abst. B* **1943**, *43*, 25; Tung, L. H. *Polymer Fractionation*; Cantow, M. J. R Ed.; Academic: New York, 1967.

28 The uncertainty ± 0.4 in temperature is estimated from the standard deviation of K as shown in Table 1 and the temperature dependence of viscosity as given in ref. 29.

29. Plazek, D. J.; O'Rourke, V. M. J. *Polym. Sci. A-2* **1971**, *9*, 209.

30. In the visual superposition to obtain a good fit, both the calculated and measured curves are first displayed in separate figures using the same scales. The figures are stored in a graphic software (CorelDRAW) which allows the superposition to be done under a large magnification on a monitor and at the same time allows the data points being plotted onto the calculated curve. The finished figures can be adjusted to any suitable size. In this procedure, logical steps can be followed to ensure that the comparison between the theory and experiments is accurate.

31 Lin, Y.-H. The accompanying paper.

32 Note: Confirmation is made by the agreement between the temperature dependence of the structural-relaxation time τ_S of sample A as defined in ref. 31–i.e. equivalent to the temperature dependence of the product of *K* and *s*–and that of *J*(*t*) in the recoverable region determined by Plazek through data reduction, as shown in Figure 5 of ref. 31. The agreement in temperature dependence between the obtained *K* values and the viscosity results of Plazek is also shown in the same figure. These agreements support the consistency between the composition of the *J*(*t*) curves measured at different temperatures as shown in Figure 1 and that shown in Figure 2 of ref. 19; the former is guided by the fittings to eqs 1, 4 and 5, while the latter was done through the data reduction by Plazek.

33 Mills, P. J.; Green, P. F.; Palmstrom, C. J.; Mayer, J. W.; Kramer, E. *J. Appl. Phys. Lett.* **1984**, *45*, 958. The measurement temperature 170^{o}C in this paper has been corrected to be 174^{o}C in ref. 35.

34 Green, P. F.; Palmstrom, C. J.; Mayer, J. W.; Kramer, E. J. *Macromolecules* **1985**, *18*, 501.

35 Green, P. F.; Kramer, E. J. *Macromolecules* **1986**, *19*, 1108.

36. Plazek, D. J. *J. Rheol.* **1996**, *40*, 987.

37 Note: The blend solution is a binary blend consisting of one nearly monodisperse component with molecular weight much higher than M_e and another with molecular weight just below M_e , which can be regarded as a solvent as far as entanglement is concerned. The details can be found in refs. 4 and 5.

38 Fetters, L. J.; Lohse, D. J.; Richter, D.; Witten, T. A.; Zirkel, A. *Macromolecules* **1994**, *27*, 4639.

39 Angell, C. A. Science **1995**, *267*, 1924; and references therein.

40 Debenedetti, P. G.; Stillinger, F. H. *Nature* **2001**, *410*, 259.

41 Plazek[20] estimated that T_g of sample B is lowered by the presence of residual plasticizers by about 1 degree. Although in general there is some uncertainty as to the measurement of the calorimetric T_g value, the value of sample A should be very close to 97.8°C, while that of sample B should be around 98.5°C. (see refs. 42 and 43)

42 Fox, T. G.; Loshaek, S. *J. Polym. Sci*. **1955**, *15*, 371.

43 Lin, Y.-H. *Macromolecules* **1990**, ***23***, 5292; and unpublished results.

44 Nemoto, N.; Odani, H.; Kurata, M. *Macromolecules* **1972**, *5*, 531.

45 Note: one may also calculate the shift $\Delta \log t$ using eq 3 of ref. 44.

46 Ninomiya, K.; Ferry,J. D. *J. Phys. Chem.* **1963**, *67*, 2292.

47 Onogi, S.; Masuda, T.; Kitagawa, K. *Macromolecules* **1970**, *3*, 109.

48 Plazek, D. J. *Polymer J*. **1980**, *12*, 43.

49 Okamoto, H.; Inoue, T.; Osaki, K. *J. Polym. Sci: Part B: Polym. Phys.* **1995**, *33*, 417..

50 Inoue, T.; Hwang, E. J.; Osaki, K. *J. Rheol.* **1992**, *36*, 1737.

51 Adachi, K.; Hirano, H. *Macromolecules* **1998**, *31*, 3958.

52. Doi, M.; Edwards, S. F. *The Theory of Polymer Dynamics*; Oxford Univ. Press: New York, 1986.

53. Lin, Y.-H. *Macromolecules* **1987**, *20*, 3080.

54 Sillescu, H. *J. Non-Crystal. Solids* **1999**, *243*, 81; and references therein.

55 Hempel, E.; Hempel, G.; Hensei, A.; Schick, C.; Donth, E. *J. Phys. Chem. B* **2000**, *104*, 2460.

56 Tracht, U.; Wilhelm, M.; Heuer, A.; Feng, H.; Schmidt-Rohr, K.; Spiess, H. W. *Phys. Rev. Lett.* **1998**, *81*, 2727.

57 Cicerone, M. T.; Blackburn, F. R.; Ediger, M. D. *J. Chem. Phys.* **1995**, *102*, 471.

58 Arndt,M.; Stannarius, R.; Groothues, E.; Hempel, E.; Kremer, F. *Phys. Rev. Lett.* **1997**, *79*, 2077.

59 Note: Strictly speaking, the fluid region of sample A at 97°C is slightly affected by the glassy-relaxation process, as show in Figure 1. The effect is more prone to occur as the molecular weight is smaller and the temperature is closer to T_g. In the case of sample A, whose molecular weight is not that low, the effect causes at most a shift of 20% along the time coordinate in the fluid region. Besides, the shift is accounted for in determining the *K* value as shown by the close fitting between the calculated and measured curves. Thus, any error that can arise is really very small.

60. Thirumalai, D.; Mountain, R. D. *Phys. Rev. E* **1993**, *47*, 479.

61. Angell, C. A. *J. Phys. Chem. Solids* **1988**, *49*, 863.

62. Stillinger, F. H. *J. Chem. Phys.* **1988**, *89*, 6461.

63. Donati C.; Glotzer, S. C.; Poole, P. H.; Kob, W.; Plimpton, S. J. *Phys. Rev. E* **1999**, *60*, 3107.

64. Weeks, E. R.; Crocker, J. C.; Levitt, A. C.; Schofield, A.; Weitz, D. A. *Science* **2000**, *287*, 627.

65 Cicerone, M. T.; Ediger, M. D. *J. Chem. Phys.* **1995**, *103*, 5684.

66 Cicerone, M. T.; Ediger, M. D. *J. Chem. Phys.* **1996**, *104*, 7210.

67 Schiener,B.; Bohmer, R.; Loidl, A.; Chamberlin, R. V. *Science* **1996**, *274*, 752.

68 Richert, R. *J. Phys. Chem. B* **1997**, *101*, 6323.

69 Russell, E. V.; Israeloff, N. E. *Nature* **2000**, *408*, 695.

70 Tracht, U.; Wilhelm, M.; Heuer, A.; Feng, H.; Schmidt-Rohr, K.; Spiess, H. W. *Phys. Rev. Lett.* **1998**, *81*, 2727.

71 Adam, G.; Gibbs, J. H. *J. Chem. Phys*. **1965**, *43*, 139.

72 Mountain, R. D. *J. Chem. Phys.* **1995**, *102*, 5408; and references therein.

73. McCrum, N. G.; Read, R. E.; Williams, G. *Anelastic and Dielectric Effects in Polymeric Solids*; Wiley: London, 1967.

74. Kovacs, A. *J. Polym. Sci.* **1958**, *30*, 131.

75. Goldstein, M. *J. Chem. Phys*. **1969**, *51*, 3728.

76. Moynihan, C. T.; Schroeder, J. *J. Non-Cryst. Solids* **1993**, *160*, 52.

77. Debenedtti, P. G.; Stillinger, F. H. *Nature* **2001**, *410*, 259.

78. Sastry, S.; Debenedetti, P. G.; Stillinger, F. H. *Nature* **1998**, *393*, 554.

79. Schroder, T. B.; Sastry, S.; Dyre, J. C.; Glotzer, S. C. *J. Chem. Phys*. **2000,** *112*, 9834.

80 Fulcher, G. S. *J. Am. Chem. Soc*., **1925**, *8*, 339, 789; Tammann, G. and Hesse, G., Z. *Anorg. Allg. Chem.* **1926**, *156*, 245.

81. Williams, M. L.; Landel, R. F.; Ferry, J. D. *J. Am. Chem. Soc.* **1955**, *77*, 3701.

82 Fujara, F.; Geil, B.; Sillescu, H.; Fleischer, G. *Z. Phys. B: Condens. Matter* **1992**, *88*, 195.

83 Cicerone, M. T.; Ediger, M. D. *J. Phys. Chem.* **1993**, *97*, 10489.

84. Kind, R.; Liechti, N.; Korner, N.; Hulliger, J. *Phys. Rev. B* **1992**, *45*, 7697.

85. Swallen, S. F.; Bonvallet, P. A.; McMahon, R. J.; Ediger, M. D. *Phys. Rev. Lett.* **2003,** *90*, 015901.

86. Fox, T. G.; Flory, P. J. *J. Appl. Phys*. **1950**, *21*, 581.

87 Cohen, M. H.; Turnbull, D. *J. Chem. Phys.* **1959**, *31*, 1164.

88 See refs. 63 and 64. Note: The similarity may have the following explanation: In a glass-forming liquid, the strength and length scale of the correlation between mobile particles are found to grow strongly with decreasing temperature. At a sufficient low temperature, at any given time, most particles are localized in cages and a small percentage of particles form large clusters of smaller, cooperatively rearranging "strings." After rearranging, these mobile particles become caged themselves, and others become mobile. In such a picture, cages represent the obstacles to mobility of particles. In an entangled polymer melt, the obstacles are represented by the "tube" of the reptation model. Because of the permanent chemical bonds in a polymer molecule, the mobile strings always stay on individual polymer chains.

89 Note: ERT is quantitatively valid only for nearly monodisperse systems. Because of the so-called tube dilation effect which has been shown to occur in the long-time region of a binary blend, ERT will gradually become not applicable when the polydispersity M_w/M_n of the sample has gone significantly beyond 1.1. See refs.5 and 90 for details.

90 Lin, Y.-H. *Macromolecules* **1989**, *22*, 3075; 3080.

91 Angell, C. A. *J. Non-Cryst. Solids* **1991**, *131-133*, 13.

92 see page 182 of ref. 5.

References and Notes of Report b (in report b, all the reference numbers smaller than 92 are to be added 92 for using the following references)

93 Rouse, P. E. Jr. *J. Chem. Phys.* **1953**, *21*, 1271.

94. Doi, M.; Edwards, S. F. *The Theory of Polymer Dynamics*; Oxford University Press: New York, 1986.

95. Bird, R. B.; Curtiss, C. F.; Armstrong, R. C.; Hassager, O. *Dynamics of Polymeric Liquids, Vol. 2, Kinetic Theory*, 2nd ed.; Wiley: New York. 1987.

96. Lin, Y.-H. *Polymer Viscoelasticity: Basics, Molecular Theories and Experiments*; World Scientific: Singapore. 2003.

97 Ferry, J. D. *Viscoelastic Properties of Polymers*, 3rd ed.; Wiley: New York, 1980

98 Inoue, T.; Okamoto, H.; Osaki, K. *Macromolecules* **1991**, *24*, 5670.

99 Inoue, T.; Hayashihara, H.; Okamoto, H.; Osaki, K. *J. Polym. Sci., Polym. Phys. Ed.* **1992**, *30*, 409.

100. Inoue, T.; Osaki, K. *Macromolecules* **1996**, *29*, 1595.

101 Lin, Y.-H. *J. Polym. Res.***1994**,*1*, 51.

102. Lin, Y.-H.; Lai, C. S. *Macromolecules* **1996**, *29*, 5200.

103. Lin, Y.-H. The first of the two papers currently presented.

104 Inoue, T.; Uematsu, T.; Osaki, K. *Macromolecules* **2002**, *35*, 820.

105. Patterson, G. D.; Lindsey, C. P.; Stevens, J. R. *J. Chem. Phys.* **1979**, *70*, 643.

106. Lin, Y.-H. *Macromolecules* **1986**, *19*, 168.

107. Lin, Y.-H.; Juang, J.-H. *Macromolecules* **1999**, *32*, 181.

108. Lin, Y.-H. *Macromolecules* **1984**, *17*, 2846.

109. Lin, Y.-H. *Macromolecules* **1986**, *19*, 159.

110. Lin, Y.-H. *Macromolecules* **1987**, *20*, 885.

111. Lin, Y.-H. *Macromolecules* **1991**, *24*, 5346.

112. Doi, M; Edwards, S. F. *J. Chem. Soc., Faraday Trans. 2* **1978**, *74*, 1789; **1978**, *74*, 1802.

113 Lai, C. S.; Juang, J.-H.; Lin, Y.-H. *J. Chem. Phys.* **1999**, *110*, 9310.

114 Lin, Y.-H.; Luo, Z.-H. *J. Chem. Phys.* **2000**, *112*, 7219.

115 Lin, Y.-H. *J. Chin. Chem. Soc.* **2002**, *49*, 629.

116. Mooney, M. *J. Polym. Sci.* **1959**, *34*, 599.

117 Doi, M. *J. Polym. Sci., Polym. Phys. Ed.* **1980**, *18*, 1005.

118. Mandel, L. *Prog. Opt.* **1963**, *2*, 181.

119. Chu, B. *Laser Light Scattering: Basic Principles and Practice*; Academic Press: San Diego, 1991.

120. Pecora, R., ed. *Dynamic Light Scattering: Application of Photon Correlation Spectroscopy*; Plenum Press: New York, 1985.

121. Berne, B. J.; Pecora, R. *Dynamic Light Scattering*; Wiley: New York, 1976.

122 Plazek, D. J.; O'Rourke, V. M. *J. Polym. Sci.A*-2 **1971**, *9*, 209.

123. Lindsey, C. P.; Patterson, G. D.; Stevens, J. R. *J. Polym. Sci., Polym. Phys. Ed.* **1979**, *17*, 1547.

124 Ballard, D. G. H.; Rayer, M. G.; Schelten, J. *Polymer* **1976**, *17*, 349.

125. Norisuye, T.; Fujita, H. *Polym. J.* **1982**, *14*, 143.

126. Fischer, E. W.; Dettenmaier, M. *J. Non-Cryst, Solids* **1978**, *31*, 181.

127. Ehrenburg, E. G.; Piskareva, E. P.; Poddubnyi, I. Y. A. *J. Polym. Sci., Polym. Symp.* **1973**, No. 42, 1021.

128. Alms, G. R.; Bauer, D. R.; Brauman, J. I.; Pecora, R. *J. Chem. Phys.* **1973**, *59*, 5310.

129. It has been shown by the Monte Carlo simulation in Ref. 22 that for the mean square length of a Rouse segment $\langle \mathbf{b}^2 \rangle$ set at 100, $\langle |\mathbf{b}| \rangle = 9.23 \approx \langle \mathbf{b}^2 \rangle^{1/2}$. On this basis, the Rouse segment and the Kuhn segment can be treated as basically equivalent to each other. In ref. 8, Inoue and Osaki have given the sizes of the Rouse segment and Kuhn segment for various polymers, showing that they are basically the same.

130 Lindsey, C. P.; Patterson, G. D. *J. Chem. Phys.* **1980**, *73*, 3348.

131 In ref 12, the *m* value is calculated from the rubbery modulus at high-frequency limit extracted from analyzing the dynamic mechanical and birefringence results. As opposed to Inoue's *m* value being calculated from a *static* quantity, the depolarized photon-correlation and viscosity data, as correlated to obtain *m*, are *dynami*c quantities.

132. Hopkins, I. L.; Hamming, R. W. *J. Appl. Phys.* **1957**, *28*, 906; **1958**, *29*, 742.

133. Tschoegl, N. W. *The Phenomenological Theory of Linear Viscoelastic Behavior*; Springer-Verlag: Berlin, 1989.

134 Plazek, D. J. *J. Phys.Chem.* **1965**, *69*, 3480.

135. Plazek, D. J. *J. Polym. Sci. A-2* **1968**, *6*, 621.

136. McCrum, N. G.; Read, B. E.; Williams, G. *Anelastic and Dielectric Effects in Polymeric Solids*, Dover: Mineola, N.Y., 1991.

137 Such a small shift between ω and $1/t$ is also indicated in page 323 of Ref. 5.

138. Note: Several factors affect the ratio between τ_v and $\langle \tau_c \rangle$: As given by eq 8 of ref. 11, the ratio of K' to K used in calculating τ_v depends on the molecular weight of the sample. Here, τ_v is for sample A whose M_w value is 4.69×10^4 (K'/K=1.61), while the $\langle \tau_c \rangle$ values obtained by Patterson *et al*.[13] are for a sample whose molecular weight should be in the

region where its K'/K ratio is at the plateau value 3.3. Experimentally $\langle \tau_c \rangle$ represents the average relaxation time of a dynamic process whose broad relaxation-time distribution (corresponding to β=0.4) may also modify its absolute magnitude.

139. Pusey, P. N.; van Megan, W. *Physica A* **1989**, *157*, 705.